ELSEVIER

Polymer 40 (1999) 3711–3727

polymer

A constitutive model in viscoelastoplasticity of glassy polymers

Aleksey D. Drozdov*

Institute for Industrial Mathematics, 4 Hanachtom Street, Beersheba 84249, Israel

Received 30 March 1998; received in revised form 1 July 1998; accepted 4 August 1998

Abstract

Constitutive equations are derived for the viscoelastoplastic response of glassy polymers under isothermal loading. The model is based on a concept of adaptive links (a version of the theory of temporary networks), where active chains are modeled as elastoplastic elements. Breakage and reformation of adaptive links reflect the viscoelastic behavior, whereas irreversible deformations of links are responsible for plastic effects. Stress–strain relations in finite viscoelastoplasticity are developed with the use of the laws of thermodynamics. These relationships are essentially simplified at small strains, when geometrical and physical nonlinearities are neglected. The model is applied to the analysis of uniaxial extension of a viscoelastoplastic bar. Fair agreement is demonstrated between experimental data for polycarbonate and poly(methyl methacrylate) at elevated temperatures and results of numerical simulation.

Keywords: Viscoelasticity; Viscoplasticity; Constitutive equations

1. Introduction

The paper is concerned with the viscoelastic and viscoplastic behavior of glassy polymers at finite and small strains. Our objective is to derive stress–strain relations which adequately reflect the physical picture of deformation, on the one hand, and which are rather simple to calculate stresses in polymeric articles with complicated geometry, on the other.

Constitutive equations in viscoelastoplasticity of polymers have attracted attention in the past three decades because of their applications in polymer engineering [1]. Despite a number of publications on this subject, it is difficult to mention a model which correctly describes observations under arbitrary nonmonotonic loading.

Following common practice, plasticity is thought of as the stress-activated nucleation of 'mobile units' and their diffusion from one position of local equilibrium to another over an energy barrier [2]. The resistance of a polymer to plastic flow is explained by intermolecular barriers to rotation of chain segments [3]. To surmount a potential barrier, a chain should acquire some energy which is determined by the current 'effective' stress. The rate of plastic strains is determined by the Eyring theory [4] of thermally activated inelastic processes.

Robertson [5] explicitly calculated the rate of plastic flow based on the presentation of a long chain as a sequence of segments with two stable rotational conformations (*trans* and *cis*).

To model viscoplastic deformations, Haward and Thackray [6] employed an Eyring dashpot connected in parallel with a Langevin spring (to give a reason for recoverable stresses) and in series with a Hookean spring (to take account of a finite instantaneous elastic modulus).

Argon [7] derived constitutive relations in viscoplasticity of glassy polymers based on an empirical formula for the activation energy. His model was discussed and generalized in several studies [8–12].

The concept of absolute reaction rates is restricted to relatively low temperatures [13]. Its extension to a region in the vicinity of the rubber–glass transition has been carried out by Ree and Eyring [14].

Bauwens-Crowet and coauthors [13,15,16] derived stress–strain relations for glassy polymers based on the Ree–Eyring theory with two stages of plastic flow (corresponding to α and β relaxation processes). Fotheringham and Cherry [2] described yield of glassy polymers by using a model with n activated rate processes, where n is an arbitrary integer. With the growth of n, their model turns into a model of cooperative relaxation [17].

G'Sell and Jonas [18] treated plastic deformation as propagation of linear molecular misfits (the so-called plastic waves) and calculated the rate of plastic strains as a product of three parameters (the mean velocity of a plastic wave, the

* Tel.: + 972-7-6231313; Fax: + 972-7-6231211.

0032-3861/99/$ - see front matter
PII: S0032-3861(98)00616-8

wave density, and an analog of the Burgers vector), which change in time in accordance with the Eyring theory.

Analogous constitutive equations were proposed in Refs. [19–21], where inelastic deformations of glassy polymers were thought of as nucleation and propagation of mobile defects. The rate of plastic flow was given by a relationship similar to the Eyring formula (thermally activated glide process), where the energy of activation was determined by the difference between the current stress and some internal stress (arising because of long-range interaction between plastic defects).

The stress–strain relations in the model of plastic defects are close to those developed in the viscoplasticity theory based on the overstress concept [22,23].

A yield-like response in tensile tests with constant rates of strains (the presence of a local maximum on the stress–strain curve, apparent softening immediately after the yield point, and hardening at relatively large strains) has been described in Refs. [24–27] in the framework of nonlinear viscoelasticity with a mechanically induced internal clock.

To describe the viscoelastoplastic behavior of glassy polymers, the present study employs a concept of temporary networks [28–31] in the version of a model of adaptive links [27,32–37]. Below the glass transition temperature, the contribution of the configurational entropy of long chains into the free energy of a network is neglected, and a polymeric material is modeled as a network of physical and chemical crosslinks connected to temporary junctions. Any crosslink is thought of as a spring (link) possessing some mechanical energy of deformations. Unlike previous studies [27,32–37] where adaptive links are treated as linear or nonlinear elastic elements, we model a link as an elastoplastic element under time-varying uniaxial tension (compression). Breakage and reformation of adaptive links in a temporary network reflect the viscoelastic effects in the bulk material, whereas irreversible deformations of individual links are responsible for the plastic effects observed at the macro-level. A constitutive model in viscoplasticity of glassy polymers, where the breakage process was incorporated with the plastic flow (but without reformation of dangling chains) has been recently proposed by Tomita and Tanaka [38].

The exposition is organized as follows. First, we introduce a model of adaptive links and develop governing equations for the numbers of links of various kinds in a temporary network. Then we calculate the potential energy of an individual chain and the strain energy density of a network. The latter expression is employed to introduce thermodynamic potentials of a transient network. We apply these potentials to derive constitutive equations for a viscoelastoplastic medium at finite strains using the laws of thermodynamics. The resulting equations are essentially nonlinear, and their employment at finite strains requires numerical simulation. The stress–strain relations are significantly simplified at small strains. To find adjustable parameters of the model and to verify the constitutive relations, we use experimental data for polycarbonate and rubber-toughened poly(methyl methacrylate). It is demonstrated that the model provides fair agreement between observations and results of numerical analysis.

2. A model of adaptive links

Conventional network theories [28–31] treat a polymer as a system of active chains connected to junctions. A chain is defined as a sequence of monomers between two adjacent crosslinks or entanglements. The points of linking (junctions) are assumed to be frozen in the bulk material (an affinity hypothesis [39]). This picture correctly describes the response of polymeric melts and solutions at elevated temperature, when the free energy of crosslinks and entanglements is negligible compared to the free energy of long chains. Since the average number of monomers in a long chain is large, the contribution of its mechanical energy into the free energy is small compared to that of the configurational entropy, and the entropic elasticity determines thermodynamic potentials of a network.

Below the glass transition temperature, the average length of a chain crucially decreases because of the growth in the number of entanglements. This entails a decrease in the configurational entropy of long chains and an increase in the mechanical energy of physical and chemical crosslinks and entanglements (adaptive links) [40,41]. The contribution of the configurational entropy of long chains into the free energy of a network becomes insignificant, whereas the effect of the potential energy of links becomes dominant (see Refs. [27,35–37]).

To predict the viscoelastic response of a polymer, we assume that M kinds of links exist that break and reform. Different kinds of links reflect interactions between long chains with different length scales. Their interrelations in an entangled polymer (when a chain suffers microstrains driven by mechanical factors with different characteristic lengths) result in a continuous spectrum of relaxation times typical of viscoelastic media. A continuous spectrum is conventionally matched by a discrete spectrum, the number M of whose elements is chosen to ensure an acceptable level of accuracy in fitting experimental data. Formally, this value may be determined based on the physical picture of interactions, when adaptive links of various kinds correspond to forces with the length scale of a monomer, an entanglement, a strand, a coil, etc. However, the simplest way is to treat M as an adjustable parameter that determines the number of points in a discrete approximation of a continuous spectrum.

The number of links (per unit mass) of the mth kind existing at the current time t, arising before a time $\tau < t$, and directed along some unit vector $\bar{l}$ at the instant of their creation is denoted as $\Xi_m(t, \tau, \bar{l})$. The functions $\Xi_m(t, \tau, \bar{l})$ generalize the chain-distribution functions introduced by

Yamamoto [29]. For example, the quantity $\Xi_m(t,0,\bar{l})$ equals the number of initial links (per unit mass) of the mth kind with the guiding vector $\bar{l}$ which exist at time t, whereas the amount

$$\frac{\partial \Xi_m}{\partial \tau}(t,\tau,\bar{l})\,d\tau$$

is the number of links which were created within the interval $[\tau,\tau+d\tau]$ with the guiding vector $\bar{l}$ and exist at the current time t.

To derive conservation laws for the functions Ξ_m, we introduce relative rates of breakage $\Gamma_m(t,\tau,\bar{l})$ and $\Gamma_{m0}(t,\bar{l})$ as the ratios of the numbers of links annihilated per unit time to the numbers of existing links:

$$\Gamma_{m0}(t,\bar{l}) = -\frac{1}{\Xi_m(t,0,\bar{l})}\frac{\partial \Xi_m}{\partial t}(t,0,\bar{l}),$$
$$\Gamma_m(t,\tau,\bar{l}) = -\left[\frac{\partial \Xi_m}{\partial \tau}(t,\tau,\bar{l})\right]^{-1}\frac{\partial^2 \Xi_m}{\partial t\,\partial \tau}(t,\tau,\bar{l}). \tag{1}$$

The relative rates of reformation $\gamma_m(\tau,\bar{l})$ are defined as the ratios of the numbers of links arising per unit time to the numbers of links existing at the initial instant:

$$\gamma_m(\tau,\bar{l}) = \frac{1}{\Xi_m(0,0,\bar{l})}\frac{\partial \Xi_m}{\partial \tau}(t,\tau,\bar{l})\Big|_{t=\tau}. \tag{2}$$

Integration of Eq. (1) implies that

$$\Xi_m(t,0,\bar{l}) = \Xi_m(0,0,\bar{l})\exp\left[-\int_0^t \Gamma_{m0}(s,\bar{l})\,ds\right],$$
$$\frac{\partial \Xi_m}{\partial \tau}(t,\tau,\bar{l}) = \frac{\partial \Xi_m}{\partial \tau}(t,\tau,\bar{l})\Big|_{t=\tau}\exp\left[-\int_\tau^t \Gamma_m(s,\tau,\bar{l})\,ds\right]. \tag{3}$$

We substitute the second expression in Eq. (3) into Eq. (2), introduce the notation

$$\Xi(\bar{l}) = \sum_{m=1}^{M}\Xi_m(0,0,\bar{l}), \quad \eta_m(\bar{l}) = \frac{\Xi_m(0,0,\bar{l})}{\Xi(\bar{l})}, \tag{4}$$

and find that

$$\Xi_m(t,0,\bar{l}) = \Xi(\bar{l})\eta_m(\bar{l})\exp\left[-\int_0^t \Gamma_{m0}(s,\bar{l})\,ds\right],$$
$$\frac{\partial \Xi_m}{\partial \tau}(t,\tau,\bar{l}) = \Xi(\bar{l})\eta_m(\bar{l})\gamma_m(\tau,\bar{l})\exp\left[-\int_\tau^t \Gamma_m(s,\tau,\bar{l})\,ds\right]. \tag{5}$$

Combining Eq. (5) with the equality

$$\Xi_m(t,t,\bar{l}) = \Xi_m(t,0,\bar{l}) + \int_0^t \frac{\partial \Xi_m}{\partial \tau}(t,\tau,\bar{l})\,d\tau, \tag{6}$$

we arrive at the formula

$$\Xi_m(t,t,\bar{l}) = \Xi(\bar{l})\eta_m(\bar{l})\Big\{\exp\left[-\int_0^t \Gamma_{m0}(s,\bar{l})\,ds\right] + \int_0^t \gamma_m(\tau,\bar{l})\exp\left[-\int_\tau^t \Gamma_m(s,\tau,\bar{l})\,ds\right]d\tau\Big\}. \tag{7}$$

Eq. (7) is similar to the balance laws for the numbers of active chains derived by Yamamoto [29] and Tanaka and Edwards [31]. The difference between our approach and conventional theories is that Eq. (7) determines the function Ξ_m of two times t and τ and the guiding vector $\bar{l}$, whereas the standard conservation equations are written for a function of time t and the end-to-end vector.

For a network with time-independent numbers of links, when

$$\Xi_m(t,t,\bar{l}) = \Xi_m(0,0,\bar{l}) = \Xi(\bar{l})\eta_m(\bar{l}), \tag{8}$$

Eq. (7) reads

$$\exp\left[-\int_0^t \Gamma_{m0}(s,\bar{l})\,ds\right] + \int_0^t \gamma_m(\tau,\bar{l})\exp\left[-\int_\tau^t \Gamma_m(s,\tau,\bar{l})\,ds\right]d\tau = 1. \tag{9}$$

Assuming the rates of breakage and reformation to be constants,

$$\gamma_m(t,\bar{l}) = \gamma_m^o(\bar{l}), \quad \Gamma_{m0}(t,\bar{l}) = \Gamma_m(t,\tau,\bar{l}) = \Gamma_m^o(\bar{l}), \tag{10}$$

we obtain from Eq. (9)

$$\frac{\gamma_m^o(\bar{l})}{\Gamma_m^o(\bar{l})} + \left[1 - \frac{\gamma_m^o(\bar{l})}{\Gamma_m^o(\bar{l})}\right]\exp\left[-\Gamma_m^o(\bar{l})t\right] = 1.$$

This equality turns into identity if and only if the rates of creation and lost coincide,

$$\gamma_m^o(\bar{l}) = \Gamma_m^o(\bar{l}). \tag{11}$$

Bearing in mind Eqs. (10) and (11), we present Eq. (5) as follows:

$$\Xi_m(t,0,\bar{l}) = \Xi(\bar{l})\eta_m(\bar{l})\exp\left[-\Gamma_m^o(\bar{l})t\right],$$
$$\frac{\partial \Xi_m}{\partial \tau}(t,\tau,\bar{l}) = \Xi(\bar{l})\eta_m(\bar{l})\Gamma_m^o(\bar{l})\exp\left[-\Gamma_m^o(\bar{l})(t-\tau)\right]. \tag{12}$$

3. Strain energy density of an elastoplastic link

The present study deals with relatively slow reformation processes, when stresses in dangling links entirely relax before the links catch new temporary junctions. This implies that the natural (stress-free) configuration of a link arising at time τ coincides with the actual configuration of the network at the instant of its creation.

Our purpose now is to determine strain energy density at the current time t for a link created at an arbitrary time τ. At the instant of its creation, the link has a small length $\delta(\tau) \ll 1$, and it is directed along a unit guiding vector $\bar{l}$. Denote by $\bar{r}_A(s)$ and $\bar{r}_B(s)$ radius vectors of the link's ends at an arbitrary time s. One can write

$$\bar{r}_A(t) = \bar{r}_A(\tau) + \bar{u}(t,\tau,\bar{r}_A(\tau)), \quad \bar{r}_B(t) = \bar{r}_B(\tau) + \bar{u}(t,\tau,\bar{r}_B(\tau)),$$

where $\bar{u}(t,\tau,\bar{r})$ is the displacement vector at point $\bar{r}$ for transition from the actual configuration of the network at time τ to its actual configuration at time t.

At the instant of creation τ, the end-to-end vector reads

$$d\bar{r}(\tau) = \bar{r}_B(\tau) - \bar{r}_A(\tau) = \delta(\tau)\bar{l}. \tag{13}$$

At the current instant t, this vector becomes

$$\begin{aligned} d\bar{r}(t) &= \bar{r}_B(t) - \bar{r}_A(t) \\ &= \delta(\tau)\bar{l} + \left[\bar{u}(t,\tau,\bar{r}_B(\tau)) - \bar{u}(t,\tau,\bar{r}_A(\tau))\right] \\ &= \delta(\tau)\bar{l} + \left[\bar{u}(t,\tau,\bar{r}_A(\tau) + \delta(\tau)\bar{l}) - \bar{u}(t,\tau,\bar{r}_A(\tau))\right]. \end{aligned} \tag{14}$$

Neglecting terms beyond the first order compared to $\delta(\tau)$, we find from Eq. (14) that

$$d\bar{r}(t) = \delta(\tau)\bar{l}\cdot\left[\hat{I} + \bar{\nabla}(\tau)\bar{u}(t,\tau)\right]. \tag{15}$$

Here $\bar{\nabla}(t)$ is the gradient operator in the actual configuration at time t, $\hat{I}$ is the unit tensor, the dot stands for inner product, and the argument $\bar{r}_A$ is omitted for simplicity.

Introducing the relative deformation gradient for transition from the actual configuration at time τ to the actual configuration at time t

$$\bar{\nabla}(\tau)\bar{r}(t) = \hat{I} + \bar{\nabla}(\tau)\bar{u}(t,\tau), \tag{16}$$

we present Eq. (15) as follows:

$$d\bar{r}(t) = \delta(\tau)\bar{l}\cdot\bar{\nabla}(\tau)\bar{r}(t) = \left[\bar{\nabla}(\tau)\bar{r}(t)\right]^{\top}\cdot\delta(\tau)\bar{l}, \tag{17}$$

where $\top$ denotes transpose.

The length of a link $ds(t)$ is calculated as

$$ds^2(t) = d\bar{r}(t)\cdot d\bar{r}(t). \tag{18}$$

Substitution of Eqs. (13) and (17) into Eq. (18) results in

$$\begin{aligned} ds^2(\tau) &= \delta^2(\tau), \\ ds^2(t) &= \delta(\tau)\bar{l}\cdot\bar{\nabla}(\tau)\bar{r}(t)\cdot\left[\bar{\nabla}(\tau)\bar{r}(t)\right]^{\top}\cdot\delta(\tau)\bar{l} \\ &= \bar{l}\cdot\hat{G}(t,\tau)\cdot\bar{l}\,ds^2(\tau), \end{aligned} \tag{19}$$

where

$$\hat{G}(t,\tau) = \bar{\nabla}(\tau)\bar{r}(t)\cdot\left[\bar{\nabla}(\tau)\bar{r}(t)\right]^{\top} \tag{20}$$

is the relative Cauchy deformation tensor for transition from the actual configuration at time τ to the actual configuration at time t.

The extension ratio $\lambda(t,\tau,\bar{l})$ for a link existing at instant t and created at time τ with a guiding vector $\bar{l}$ is given by

$$\lambda(t,\tau,\bar{l}) = \frac{ds(t)}{ds(\tau)}. \tag{21}$$

Substitution of Eq. (19) into Eq. (21) yields

$$\lambda(t,\tau,\bar{l}) = \left[\bar{l}\cdot\hat{G}(t,\tau)\cdot\bar{l}\right]^{\frac{1}{2}}. \tag{22}$$

An adaptive link is modeled as an elastoplastic bar subjected to uniaxial extension. At the instant of its creation τ, the bar is in its natural state, and plastic deformation vanishes. During the loading process, some plastic strain is maintained. As a result, the unloaded configuration of a link at the current time t differs from its initial configuration. Denote by $ds_p(t,\tau,\bar{l})$ length of a link, created at time τ with the guiding vector $\bar{l}$, in the unloaded configuration at time t, and by

$$\lambda_p(t,\tau,\bar{l}) = \frac{ds_p(t,\tau,\bar{l})}{ds(\tau,\bar{l})} \tag{23}$$

the plastic extension ratio. It follows from Eqs. (21) and (23) that

$$\lambda(t,\tau,\bar{l}) = \frac{ds(t,\bar{l})}{ds_p(t,\tau,\bar{l})}\frac{ds_p(t,\tau,\bar{l})}{ds(\tau,\bar{l})} = \lambda_e(t,\tau,\bar{l})\lambda_p(t,\tau,\bar{l}), \tag{24}$$

where

$$\lambda_e = \frac{ds(t,\bar{l})}{ds_p(t,\tau,\bar{l})} \tag{25}$$

is the elastic extension ratio. Combining Eqs. (22) and (24), we arrive at the formula

$$\lambda_e(t,\tau,\bar{l}) = \lambda_p^{-1}(t,\tau,\bar{l})\left[\bar{l}\cdot\hat{G}(t,\tau)\cdot\bar{l}\right]^{\frac{1}{2}}. \tag{26}$$

The mechanical energy $w_m(t,\tau,\bar{l})$ of an elastoplastic link of the mth kind is assumed to be a function of the elastic extension ratio λ_e:

$$w_m(t,\tau,\bar{l}) = w_m^o\left(\lambda_e(t,\tau,\bar{l})\right). \tag{27}$$

The function $w_m^o(\lambda)$ satisfies the conditions

$$w_m^o(1) = 0, \quad \frac{dw_m^o}{d\lambda}(1) = 0. \tag{28}$$

The first equality in Eq. (28) means that the potential energy vanishes when a link is in its unloaded configuration; the second equality in Eq. (28) implies that the stress vanishes in the unloaded configuration. Substitution of Eq. (26) into Eq. (27) results in

$$w_m(t,\tau,\bar{l}) = w_m^o\left(\frac{\left[\bar{l}\cdot\hat{G}(t,\tau)\cdot\bar{l}\right]^{\frac{1}{2}}}{\lambda_p(t,\tau,\bar{l})}\right). \tag{29}$$

It follows from Eq. (29) that the derivative of the strain

energy $w_m(t,\tau,\bar{l})$ with respect to time t is calculated as

$$\frac{\partial w_m}{\partial t}(t,\tau,\bar{l}) = \frac{\mathrm{d}w_m^o}{\mathrm{d}\lambda}\left(\frac{\left[\bar{l}\cdot\hat{G}(t,\tau)\cdot\bar{l}\right]^{\frac{1}{2}}}{\lambda_p(t,\tau,\bar{l})}\right)\frac{\partial}{\partial t}\left(\frac{\left[\bar{l}\cdot\hat{G}(t,\tau)\cdot\bar{l}\right]^{\frac{1}{2}}}{\lambda_p(t,\tau,\bar{l})}\right)$$

$$= \frac{1}{\lambda_p(t,\tau,\bar{l})}\frac{\mathrm{d}w_m^o}{\mathrm{d}\lambda}\left(\frac{\left[\bar{l}\cdot\hat{G}(t,\tau)\cdot\bar{l}\right]^{\frac{1}{2}}}{\lambda_p(t,\tau,\bar{l})}\right)$$

$$\times\left\{\frac{1}{2}\left[\bar{l}\cdot\hat{G}(t,\tau)\cdot\bar{l}\right]^{-\frac{1}{2}}\left[\bar{l}\cdot\frac{\partial\hat{G}}{\partial t}(t,\tau)\cdot\bar{l}\right]\right.$$

$$\left.-\frac{\left[\bar{l}\cdot\hat{G}(t,\tau)\cdot\bar{l}\right]^{\frac{1}{2}}}{\lambda_p(t,\tau,\bar{l})}\frac{\partial\lambda_p}{\partial t}(t,\tau,\bar{l})\right\}. \tag{30}$$

The velocity vector $\bar{v}(t)$ is given by

$$\bar{v}(t) = \frac{\partial\bar{r}}{\partial t}(t). \tag{31}$$

Applying the gradient operator to Eq. (31) and changing the order of differentiation, we obtain

$$\frac{\partial}{\partial t}\bar{\nabla}(\tau)\bar{r}(t) = \bar{\nabla}(\tau)\bar{v}(t). \tag{32}$$

Since

$$\bar{\nabla}(\tau) = \bar{\nabla}(\tau)\bar{r}(t)\cdot\bar{\nabla}(t), \tag{33}$$

Eq. (32) reads

$$\frac{\partial}{\partial t}\bar{\nabla}(\tau)\bar{r}(t) = \bar{\nabla}(\tau)\bar{r}(t)\cdot\bar{\nabla}(t)\bar{v}(t) = \bar{\nabla}(\tau)\bar{r}(t)\cdot\hat{L}(t), \tag{34}$$

where

$$\hat{L}(t) = \bar{\nabla}(t)\bar{v}(t) \tag{35}$$

is the velocity gradient. We differentiate Eq. (20) with respect to time, use Eq. (34), and find that

$$\frac{\partial\hat{G}}{\partial t}(t,\tau) = \left[\frac{\partial}{\partial t}\bar{\nabla}(\tau)\bar{r}(t)\right]\cdot\left[\bar{\nabla}(\tau)\bar{r}(t)\right]^{\top}$$

$$+\ \bar{\nabla}(\tau)\bar{r}(t)\cdot\left[\frac{\partial}{\partial t}\bar{\nabla}(\tau)\bar{r}(t)\right]^{\top}$$

$$= \bar{\nabla}(\tau)\bar{r}(t)\cdot\hat{L}(t)\cdot\left[\bar{\nabla}(\tau)\bar{r}(t)\right]^{\top} + \bar{\nabla}(\tau)\bar{r}(t)\cdot\hat{L}^{\top}(t)\cdot\left[\bar{\nabla}(\tau)\bar{r}(t)\right]^{\top}$$

$$= 2\,\bar{\nabla}(\tau)\bar{r}(t)\cdot\hat{D}(t)\cdot\left[\bar{\nabla}(\tau)\bar{r}(t)\right]^{\top}, \tag{36}$$

where

$$\hat{D}(t) = \frac{1}{2}\left[\hat{L}(t) + \hat{L}^{\top}(t)\right] \tag{37}$$

is the rate-of-strain tensor. It follows from Eq. (36) that

$$\bar{l}\cdot\frac{\partial\hat{G}}{\partial t}(t,\tau)\cdot\bar{l} = 2\bar{l}\cdot\bar{\nabla}(\tau)\bar{r}(t)\cdot\hat{D}(t)\cdot\left[\bar{\nabla}(\tau)\bar{r}(t)\right]^{\top}\cdot\bar{l}$$

$$= 2\hat{\mathscr{F}}(t,\tau,\bar{l}) : \hat{D}(t), \tag{38}$$

where

$$\hat{\mathscr{F}}(t,\tau,\bar{l}) = \left[\bar{\nabla}(\tau)\bar{r}(t)\right]^{\top}\cdot\overline{\bar{l}\bar{l}}\cdot\bar{\nabla}(\tau)\bar{r}(t) \tag{39}$$

is the generalized relative Finger tensor, $\overline{\bar{l}\bar{l}}$ is the dual product of the guiding vector $\bar{l}$ by itself, and the colon denotes convolution of tensors. The conventional relative Finger tensor $\hat{F}(t,\tau)$ for transition from the actual configuration at time τ to the actual configuration at time t is obtained from Eq. (39), provided the tensor $\overline{\bar{l}\bar{l}}$ is replaced by the unit tensor $\hat{I}$,

$$\hat{F}(t,\tau) = \left[\bar{\nabla}(\tau)\bar{r}(t)\right]^{\top}\cdot\bar{\nabla}(\tau)\bar{r}(t). \tag{40}$$

Substituting Eq. (38) into Eq. (30), we arrive at the formula

$$\frac{\partial w_m}{\partial t}(t,\tau,\bar{l}) = \frac{1}{\lambda_p(t,\tau,\bar{l})}\frac{\mathrm{d}w_m^o}{\mathrm{d}\lambda}\left(\frac{\left[\bar{l}\cdot\hat{G}(t,\tau)\cdot\bar{l}\right]^{\frac{1}{2}}}{\lambda_p(t,\tau,\bar{l})}\right)$$

$$\times\left\{\left[\bar{l}\cdot\hat{G}(t,\tau)\cdot\bar{l}\right]^{-\frac{1}{2}}\hat{\mathscr{F}}(t,\tau,\bar{l}) : \hat{D}(t)\right.$$

$$\left.-\frac{\left[\bar{l}\cdot\hat{G}(t,\tau)\cdot\bar{l}\right]^{\frac{1}{2}}}{\lambda_p(t,\tau,\bar{l})}\frac{\partial\lambda_p}{\partial t}(t,\tau,\bar{l})\right\}. \tag{41}$$

4. Strain energy density of a temporary network

To simplify calculations, we confine ourselves to incompressible viscoelastoplastic media. In this case, we can neglect the energy of interaction between adaptive links [31] and calculate the specific potential energy of adaptive links (per unit mass) as a sum of the mechanical energies of links existing at the current time t:

$$W(t) = \sum_{m=1}^{M}\int_{\mathscr{S}}\left[\Xi_m(t,0,\bar{l})w_m(t,0,\bar{l})\right.$$

$$\left.+\int_0^t\frac{\partial\Xi_m}{\partial\tau}(t,\tau,\bar{l})w_m(t,\tau,\bar{l})\,\mathrm{d}\tau\right]\mathrm{d}A(\bar{l}), \tag{42}$$

where $\mathscr{S}$ is a unit sphere in the space of guiding vectors $\bar{l}$, and $\mathrm{d}A(\bar{l})$ is an area element on $\mathscr{S}$. Substituting Eqs. (5) and

(29) into Eq. (42), we find that

$$W(t)=\sum_{m=1}^{M}\int_{\mathscr{S}}\eta_m(\bar{l})\Big\{\exp\Big[-\int_0^t\Gamma_{m0}(s,\bar{l})\,\mathrm{d}s\Big]\times w_m^o\left(\frac{\Big[\bar{l}\cdot\hat{G}_0(t)\cdot\bar{l}\Big]^{\frac{1}{2}}}{\lambda_{p0}(t,\bar{l})}\right)+\int_0^t\gamma_m(\tau,\bar{l})\times\exp\Big[-\int_\tau^t\Gamma_m(s,\tau,\bar{l})\,\mathrm{d}s\Big]w_m^o\left(\frac{\Big[\bar{l}\cdot\hat{G}(t,\tau)\cdot\bar{l}\Big]^{\frac{1}{2}}}{\lambda_p(t,\tau,\bar{l})}\right)\times\mathrm{d}\tau\Big\}\Xi(\bar{l})\,\mathrm{d}A(\bar{l}),\tag{43}$$

where

$$\hat{G}_0(t)=\bar{\nabla}_0\bar{r}(t)\cdot\big[\bar{\nabla}_0\bar{r}(t)\big]^{\top}\tag{44}$$

is the Cauchy deformation tensor for transition from the initial to the actual configuration, $\bar{\nabla}_0$ is the gradient operator in the initial configuration, and $\lambda_{p0}(t,\bar{l})$ is the plastic extension ratio at time t for initial links with the guiding vector $\bar{l}$.

We differentiate Eq. (43) with respect to time t, take into account that

$$\hat{G}(t,t)=\hat{I},\quad \lambda_p(t,t,\bar{l})=1,\tag{45}$$

use Eq. (28), and obtain

$$\frac{\mathrm{d}W}{\mathrm{d}t}(t)=-\mathscr{D}_1(t)+\sum_{m=1}^{M}\int_{\mathscr{S}}\eta_m(\bar{l})\times\Big\{\exp\Big[-\int_0^t\Gamma_{m0}(s,\bar{l})\,\mathrm{d}s\Big]\frac{\partial w_m}{\partial t}(t,0,\bar{l})+\int_0^t\gamma_m(\tau,\bar{l})\times\exp\Big[-\int_\tau^t\Gamma_m(s,\tau,\bar{l})\,\mathrm{d}s\Big]\frac{\partial w_m}{\partial t}(t,\tau,\bar{l})\,\mathrm{d}\tau\Big\}\Xi(\bar{l})\,\mathrm{d}A(\bar{l}),\tag{46}$$

where

$$\mathscr{D}_1(t)=\sum_{m=1}^{M}\int_{\mathscr{S}}\eta_m(\bar{l})\Big\{\Gamma_{m0}(t,\bar{l})\exp\Big[-\int_0^t\Gamma_{m0}(s,\bar{l})\,\mathrm{d}s\Big]\times w_m^o\left(\frac{\Big[\bar{l}\cdot\hat{G}_0(t)\cdot\bar{l}\Big]^{\frac{1}{2}}}{\lambda_{p0}(t,\bar{l})}\right)+\int_0^t\gamma_m(\tau,\bar{l})\Gamma_m(t,\tau,\bar{l})\times\exp\Big[-\int_\tau^t\Gamma_m(s,\tau,\bar{l})\,\mathrm{d}s\Big]\times w_m^o\left(\frac{\Big[\bar{l}\cdot\hat{G}(t,\tau)\cdot\bar{l}\Big]^{\frac{1}{2}}}{\lambda_p(t,\tau,\bar{l})}\right)\mathrm{d}\tau\Big\}\Xi(\bar{l})\,\mathrm{d}A(\bar{l}).\tag{47}$$

Eqs. (41) and (46) imply that

$$\frac{\mathrm{d}W}{\mathrm{d}t}(t)=-\mathscr{D}_1(t)-\mathscr{D}_2(t)+\Big\langle\sum_{m=1}^{M}\int_{\mathscr{S}}\eta_m(\bar{l})\Big\{\exp\Big[-\int_0^t\Gamma_{m0}(s,\bar{l})\,\mathrm{d}s\Big]\times\frac{\mathrm{d}w_m^o}{\mathrm{d}\lambda}\left(\frac{\Big[\bar{l}\cdot\hat{G}_0(t)\cdot\bar{l}\Big]^{\frac{1}{2}}}{\lambda_{p0}(t,\bar{l})}\right)\frac{\hat{\mathscr{F}}_0(t,\bar{l})}{\lambda_{p0}(t,\bar{l})\Big[\bar{l}\cdot\hat{G}_0(t)\cdot\bar{l}\Big]^{\frac{1}{2}}}+\int_0^t\gamma_m(\tau,\bar{l})\exp\Big[-\int_\tau^t\Gamma_m(s,\tau,\bar{l})\,\mathrm{d}s\Big]\mathrm{d}\tau\times\frac{\mathrm{d}w_m^o}{\mathrm{d}\lambda}\left(\frac{\Big[\bar{l}\cdot\hat{G}(t,\tau)\cdot\bar{l}\Big]^{\frac{1}{2}}}{\lambda_p(t,\tau,\bar{l})}\right)\frac{\hat{\mathscr{F}}(t,\tau,\bar{l})}{\lambda_p(t,\tau,\bar{l})\Big[\bar{l}\cdot\hat{G}(t,\tau)\cdot\bar{l}\Big]^{\frac{1}{2}}}\Big\}\times\Xi(\bar{l})\,\mathrm{d}A(\bar{l})\Big\rangle:\hat{D}(t),\tag{48}$$

where

$$\mathscr{D}_2(t)=\sum_{m=1}^{M}\int_{\mathscr{S}}\eta_m(\bar{l})\Big\{\exp\Big[-\int_0^t\Gamma_{m0}(s,\bar{l})\,\mathrm{d}s\Big]\times\frac{\mathrm{d}w_m^o}{\mathrm{d}\lambda}\left(\frac{\Big[\bar{l}\cdot\hat{G}_0(t)\cdot\bar{l}\Big]^{\frac{1}{2}}}{\lambda_{p0}(t,\bar{l})}\right)\frac{\Big[\bar{l}\cdot\hat{G}_0(t)\cdot\bar{l}\Big]^{\frac{1}{2}}}{\lambda_{p0}^2(t,\bar{l})}\frac{\partial\lambda_{p0}}{\partial t}(t,\bar{l})+\int_0^t\gamma_m(\tau,\bar{l})\exp\Big[-\int_\tau^t\Gamma_m(s,\tau,\bar{l})\,\mathrm{d}s\Big]\times\frac{\mathrm{d}w_m^o}{\mathrm{d}\lambda}\left(\frac{\Big[\bar{l}\cdot\hat{G}(t,\tau)\cdot\bar{l}\Big]^{\frac{1}{2}}}{\lambda_p(t,\tau,\bar{l})}\right)\frac{\Big[\bar{l}\cdot\hat{G}(t,\tau)\cdot\bar{l}\Big]^{\frac{1}{2}}}{\lambda_p^2(t,\tau,\bar{l})}\frac{\partial\lambda_p}{\partial t}(t,\tau,\bar{l})\times\mathrm{d}\tau\Big\}\Xi(\bar{l})\,\mathrm{d}A(\bar{l})\tag{49}$$

and

$$\hat{\mathscr{F}}_0(t,\bar{l})=\big[\bar{\nabla}_0\bar{r}(t)\big]^{\top}\cdot\bar{l}\bar{l}\cdot\bar{\nabla}_0\bar{r}(t).\tag{50}$$

At uniaxial extension, the stress $\Sigma_m(t,\tau,\bar{l})$ in an adaptive link of the mth kind existing at time t and arising at time τ with the guiding vector $\bar{l}$ is given by the formula [42]

$$\Sigma_m(t,\tau,\bar{l})=\lambda_e(t,\tau,\bar{l})\frac{\mathrm{d}w_m^o}{\mathrm{d}\lambda}(\lambda_e(t,\tau,\bar{l})).\tag{51}$$

It follows from Eqs. (26) and (51) that

$$\frac{\mathrm{d}w_m^o}{\mathrm{d}\lambda}\left(\frac{\Big[\bar{l}\cdot\hat{G}(t,\tau)\cdot\bar{l}\Big]^{\frac{1}{2}}}{\lambda_p(t,\tau,\bar{l})}\right)=\frac{\lambda_p(t,\tau,\bar{l})}{\Big[\bar{l}\cdot\hat{G}(t,\tau)\cdot\bar{l}\Big]^{\frac{1}{2}}}\Sigma_m(t,\tau,\bar{l}).\tag{52}$$

Substitution of Eq. (52) into Eq. (49) results in

$$\mathscr{D}_2(t) = \int_{\mathscr{S}} \Bigg\{ \frac{1}{\lambda_{p0}(t,\bar{l})} \frac{\partial \lambda_{p0}}{\partial t}(t,\bar{l}) \times \sum_{m=1}^{M} \eta_m(\bar{l}) \exp\Big[-\int_0^t \Gamma_{m0}(s,\bar{l})\, \mathrm{d}s \Big] \Sigma_{m0}(t,\bar{l}) + \int_0^t \frac{1}{\lambda_p(t,\tau,\bar{l})} \frac{\partial \lambda_p}{\partial t}(t,\tau,\bar{l}) \times \sum_{m=1}^{M} \eta_m(\bar{l}) \gamma_m(\tau,\bar{l}) \exp\Big[-\int_\tau^t \Gamma_m(s,\tau,\bar{l})\, \mathrm{d}s \Big] \Sigma_m(t,\tau,\bar{l})\, \mathrm{d}\tau \Bigg\} \times \Xi(\bar{l})\, \mathrm{d}A(\bar{l}), \tag{53}$$

where $\Sigma_{m0}(t,\bar{l})$ is the stress at the current time t in an initial link of the mth kind with the guiding vector $\bar{l}$.

To transform Eq. (53), we introduce the plastic Hencky strain

$$\varepsilon_p(t,\tau,\bar{l}) = \ln \lambda_p(t,\tau,\bar{l}) \tag{54}$$

and the resulting stresses

$$\Sigma_0(t,\bar{l}) = \sum_{m=1}^{M} \eta_m(\bar{l}) \exp\Big[-\int_0^t \Gamma_{m0}(s,\bar{l})\, \mathrm{d}s \Big] \Sigma_{m0}(t,\bar{l}),$$

$$\Sigma(t,\tau,\bar{l}) = \sum_{m=1}^{M} \eta_m(\bar{l}) \gamma_m(\tau,\bar{l}) \times \exp\Big[-\int_\tau^t \Gamma_m(s,\tau,\bar{l})\, \mathrm{d}s \Big] \Sigma_m(t,\tau,\bar{l}). \tag{55}$$

In the new notation, Eq. (53) is written as follows:

$$\mathscr{D}_2(t) = \int_{\mathscr{S}} \Bigg\{ \frac{\partial \varepsilon_{p0}}{\partial t}(t,\bar{l}) \Sigma_0(t,\bar{l}) + \int_0^t \frac{\partial \varepsilon_p}{\partial t}(t,\tau,\bar{l}) \Sigma(t,\tau,\bar{l}) \mathrm{d}\tau \Bigg\} \Xi(\bar{l})\, \mathrm{d}A(\bar{l}). \tag{56}$$

5. Thermodynamic potentials and constitutive equations

The first law of thermodynamics [43] reads

$$\frac{\mathrm{d}\Phi}{\mathrm{d}t} = \frac{1}{\rho}\big(\hat{\sigma} : \hat{D} - \bar{\nabla}\cdot\bar{q}\big) + r. \tag{57}$$

Here Φ is the specific internal energy per unit mass, $\bar{q}$ is the heat flux vector, r is the heat supply per unit mass, ρ is a constant mass density, and $\hat{\sigma}$ is the Cauchy stress tensor.

We present the stress tensor $\hat{\sigma}$ as a sum of its spherical and deviatoric components,

$$\hat{\sigma} = -p\hat{I} + \hat{s}, \tag{58}$$

where p is pressure, substitute Eq. (58) into Eq. (57), use the incompressibility condition

$$I_1(\hat{D}) = 0, \tag{59}$$

and obtain

$$\frac{\mathrm{d}\Phi}{\mathrm{d}t} = \frac{1}{\rho}\big(\hat{s} : \hat{D} - \bar{\nabla}\cdot\bar{q}\big) + r. \tag{60}$$

The Clausius–Duhem inequality [43] implies that

$$\rho\frac{\mathrm{d}\mathscr{Q}}{\mathrm{d}t} = \rho\frac{\mathrm{d}S}{\mathrm{d}t} + \bar{\nabla}\cdot\Big(\frac{\bar{q}}{\Theta}\Big) - \frac{\rho r}{\Theta} \geq 0, \tag{61}$$

where S is the specific entropy (per unit mass), $\mathscr{Q}$ is the specific entropy production, and Θ is the absolute temperature. Bearing in mind that

$$\bar{\nabla}\cdot\Big(\frac{\bar{q}}{\Theta}\Big) = \frac{1}{\Theta}\bar{\nabla}\cdot\bar{q} - \frac{1}{\Theta^2}\bar{q}\cdot\bar{\nabla}\Theta,$$

and excluding the term $\bar{\nabla}\cdot\bar{q}$ from Eqs. (60) and (61), we arrive at the formula

$$\Theta\frac{\mathrm{d}\mathscr{Q}}{\mathrm{d}t} = \Theta\frac{\mathrm{d}S}{\mathrm{d}t} - \frac{\mathrm{d}\Phi}{\mathrm{d}t} + \frac{1}{\rho}\Big(\hat{s} : \hat{D} - \frac{1}{\Theta}\bar{q}\cdot\bar{\nabla}\Theta\Big) \geq 0. \tag{62}$$

Taking into account that

$$\Phi = \Psi + S\Theta, \tag{63}$$

where Ψ is the specific free (Helmholtz) energy, we present Eq. (62) in the form

$$\Theta\frac{\mathrm{d}\mathscr{Q}}{\mathrm{d}t} = -S\frac{\mathrm{d}\Theta}{\mathrm{d}t} - \frac{\mathrm{d}\Psi}{\mathrm{d}t} + \frac{1}{\rho}\Big(\hat{s} : \hat{D} - \frac{1}{\Theta}\bar{q}\cdot\bar{\nabla}\Theta\Big) \geq 0. \tag{64}$$

We accept the following expressions for the specific free energy and the specific entropy:

$$\Psi = \Psi^o + (c - S^o)(\Theta - \Theta^o) - c\Theta\ln\frac{\Theta}{\Theta^o} + W, \tag{65}$$

$$S = S^o + c\ln\frac{\Theta}{\Theta^o}. \tag{66}$$

Here Ψ^o and S^o are the specific free energy and the specific entropy in the initial (stress-free) configuration at the reference temperature Θ^o, and c is the specific heat capacity (per unit mass) of adaptive links. Confining ourselves to processes with weakly varying temperature Θ, we suppose that the parameters Ψ^o, S^o, and c are constants.

Substituting Eqs. (48), (65) and (66) into Eq. (64), we find

that

$$\rho\Theta(t)\frac{\mathrm{d}\mathscr{Q}}{\mathrm{d}t}(t)=\rho[\mathscr{D}_1(t)+\mathscr{D}_2(t)]-\frac{1}{\Theta(t)}\bar{q}(t)\cdot\bar{\nabla}(t)\Theta(t)$$
$$+\hat{D}(t):\Big\langle\hat{s}(t)-\rho\sum_{m=1}^{M}\int_{\mathscr{S}}\eta_m(\bar{l})\Big\{\exp\Big[-\int_0^t\Gamma_{m0}(s,\bar{l})\,\mathrm{d}s\Big]$$
$$\times\frac{\mathrm{d}w_m^o}{\mathrm{d}\lambda}\left(\frac{\Big[\bar{l}\cdot\hat{G}_0(t)\cdot\bar{l}\Big]^{\frac{1}{2}}}{\lambda_{p0}(t,\bar{l})}\right)\frac{\hat{\mathscr{F}}_0(t,\bar{l})}{\lambda_{p0}(t,\bar{l})\Big[\bar{l}\cdot\hat{G}_0(t)\cdot\bar{l}\Big]^{\frac{1}{2}}}$$
$$+\int_0^t\gamma_m(\tau,\bar{l})\exp\Big[-\int_\tau^t\Gamma_m(s,\tau,\bar{l})\,\mathrm{d}s\Big]\mathrm{d}\tau$$
$$\times\frac{\mathrm{d}w_m^o}{\mathrm{d}\lambda}\left(\frac{\Big[\bar{l}\cdot\hat{G}(t,\tau)\cdot\bar{l}\Big]^{\frac{1}{2}}}{\lambda_p(t,\tau,\bar{l})}\right)\frac{\hat{\mathscr{F}}(t,\tau,\bar{l})}{\lambda_p(t,\tau,\bar{l})\Big[\bar{l}\cdot\hat{G}(t,\tau)\cdot\bar{l}\Big]^{\frac{1}{2}}}\Big\}$$
$$\times\Xi(\bar{l})\,\mathrm{d}A(\bar{l})\Big\rangle\geq 0. \tag{67}$$

Following common practice, we equate terms in the angle brackets to zero, use Eq. (58), and obtain the constitutive equation

$$\hat{\sigma}(t)=-p(t)\hat{I}+\rho\sum_{m=1}^{M}\int_{\mathscr{S}}\eta_m(\bar{l})\Big\{\exp\Big[-\int_0^t\Gamma_{m0}(s,\bar{l})\,\mathrm{d}s\Big]$$
$$\times\frac{\mathrm{d}w_m^o}{\mathrm{d}\lambda}\left(\frac{\Big[\bar{l}\cdot\hat{G}_0(t)\cdot\bar{l}\Big]^{\frac{1}{2}}}{\lambda_{p0}(t,\bar{l})}\right)\frac{\hat{\mathscr{F}}_0(t,\bar{l})}{\lambda_{p0}(t,\bar{l})\Big[\bar{l}\cdot\hat{G}_0(t)\cdot\bar{l}\Big]^{\frac{1}{2}}}$$
$$+\int_0^t\gamma_m(\tau,\bar{l})\exp\Big[-\int_\tau^t\Gamma_m(s,\tau,\bar{l})\,\mathrm{d}s\Big]\mathrm{d}\tau$$
$$\times\frac{\mathrm{d}w_m^o}{\mathrm{d}\lambda}\left(\frac{\Big[\bar{l}\cdot\hat{G}(t,\tau)\cdot\bar{l}\Big]^{\frac{1}{2}}}{\lambda_p(t,\tau,\bar{l})}\right)\frac{\hat{\mathscr{F}}(t,\tau,\bar{l})}{\lambda_p(t,\tau,\bar{l})\Big[\bar{l}\cdot\hat{G}(t,\tau)\cdot\bar{l}\Big]^{\frac{1}{2}}}\Big\}$$
$$\times\Xi(\bar{l})\,\mathrm{d}A(\bar{l}). \tag{68}$$

Combining Eqs. (67) and (68), we arrive at the formula

$$\Theta(t)\frac{\mathrm{d}\mathscr{Q}}{\mathrm{d}t}(t)=\mathscr{D}_1(t)+\mathscr{D}_2(t)-\frac{1}{\rho\Theta(t)}\bar{q}(t)\cdot\bar{\nabla}(t)\Theta(t)\geq 0. \tag{69}$$

Eq. (47) implies that the functional $\mathscr{D}_1(t)$ is nonnegative, since the concentrations η_m, the strain energies w_m^o, and the rates of reformation γ_m are nonnegative. The third term on the left-hand side of Eq. (69) is nonnegative, provided that the heat flux vector $\bar{q}$ obeys the Fourier law

$$\bar{q}(t)=-\kappa\bar{\nabla}(t)\Theta(t) \tag{70}$$

with a nonnegative thermal diffusivity κ. As a result, we find that the Clausius–Duhem inequality Eq. (69) holds if the functional $\mathscr{D}_2(t)$ is nonnegative. It follows from Eq. (56) that this assumption is valid if the rate of plastic strain satisfies the equation

$$\frac{\partial\varepsilon_p}{\partial t}(t,\tau,\bar{l})=\mathscr{H}\big(\Sigma(t,\tau,\bar{l})\big), \tag{71}$$

where $\mathscr{H}$ is an arbitrary odd function.

Eqs. (68), (70) and (71) provide constitutive equations for incompressible viscoelastoplastic media derived within the concept of temporary polymeric networks. Eq. (71) may be treated as the simplest version of constitutive relations for the rate of plastic strain which are compatible with the dissipation inequality. To generalize this relationship, one can assume that the function $\mathscr{H}$ depends also on the plastic Hencky strain $\varepsilon_p(t,\tau)$ and any objective measure of deformations. As examples, the following equations are suggested:

$$\frac{\partial\varepsilon_p}{\partial t}(t,\tau,\bar{l})=\mathscr{H}\Big(\Sigma(t,\tau,\bar{l}),\varepsilon_p(t,\tau)\Big),$$
$$\frac{\partial\varepsilon_p}{\partial t}(t,\tau,\bar{l})=\mathscr{H}\Big(\Sigma(t,\tau,\bar{l}),\varepsilon_p(t,\tau,\bar{l}),\hat{F}(t,\tau)\Big), \tag{72}$$
$$\frac{\partial\varepsilon_p}{\partial t}(t,\tau,\bar{l})=\mathscr{H}\Big(\Sigma(t,\tau,\bar{l}),\varepsilon_p(t,\tau,\bar{l}),\hat{\mathscr{F}}(t,\tau,\bar{l})\Big).$$

The only restriction imposed on the function $\mathscr{H}$ is that it should be positive and odd in the first argument Σ.

Eq. (68) is a new stress–strain relation for viscoelastoplastic polymer materials. In the limiting case of purely viscoelastic deformations, when

$$\lambda_{p0}(t,\bar{l})=1,\quad \lambda_p(t,\tau,\bar{l})=1, \tag{73}$$

Eq. (68) turns into the constitutive equation for nonlinear viscoelastic media [44].

Substituting Eq. (52) into Eq. (68), we find that

$$\hat{\sigma}(t)=-p(t)\hat{I}+\rho\sum_{m=1}^{M}\int_{\mathscr{S}}\eta_m(\bar{l})\Big\{\exp\Big[-\int_0^t\Gamma_{m0}(s,\bar{l})\,\mathrm{d}s\Big]$$
$$\times\frac{\Sigma_{m0}(t,\bar{l})}{\bar{l}\cdot\hat{G}_0(t)\cdot\bar{l}}\hat{\mathscr{F}}_0(t,\bar{l})+\int_0^t\gamma_m(\tau,\bar{l})\exp\Big[-\int_\tau^t\Gamma_m(s,\tau,\bar{l})\,\mathrm{d}s\Big]$$
$$\times\frac{\Sigma_m(t,\tau,\bar{l})}{\bar{l}\cdot\hat{G}(t,\tau)\cdot\bar{l}}\hat{\mathscr{F}}(t,\tau,\bar{l})\,\mathrm{d}\tau\Big\}\Xi(\bar{l})\,\mathrm{d}A(\bar{l}). \tag{74}$$

It follows from Eqs. (55) and (74) that

$$\hat{\sigma}(t)=-p(t)\hat{I}+\rho\int_{\mathscr{S}}\left[\frac{\Sigma_0(t,\bar{l})}{\bar{l}\cdot\hat{G}_0(t)\cdot\bar{l}}\hat{\mathscr{F}}_0(t,\bar{l})\right.$$
$$\left.+\int_0^t\frac{\Sigma(t,\tau,\bar{l})}{\bar{l}\cdot\hat{G}(t,\tau)\cdot\bar{l}}\hat{\mathscr{F}}(t,\tau,\bar{l})\,\mathrm{d}\tau\right]\Xi(\bar{l})\,\mathrm{d}A(\bar{l}). \tag{75}$$

For an isotropic network with

$$\Xi(\bar{l})=\Xi, \tag{76}$$

Eq. (75) reads

$$\hat{\sigma}(t) = -p(t)\hat{I} + \rho\Xi\left\{\int_{\mathscr{S}} \frac{\Sigma_0(t,\bar{l})}{\bar{l}\cdot\hat{G}_0(t)\cdot\bar{l}}\hat{\mathscr{F}}_0(t,\bar{l})\,\mathrm{d}A(\bar{l}) + \int_0^t\left[\int_{\mathscr{S}} \frac{\Sigma(t,\tau,\bar{l})}{\bar{l}\cdot\hat{G}(t,\tau)\cdot\bar{l}}\hat{\mathscr{F}}(t,\tau,\bar{l})\,\mathrm{d}A(\bar{l})\right]\mathrm{d}\tau\right\}. \quad (77)$$

Eq. (77) is a new constitutive relation for a viscoelastoplastic medium at finite strains.

6. Constitutive equations for linear isotropic media

In this section we confine ourselves to small deformations of an isotropic polymer from the initial configuration to the actual configuration, when nonlinear terms may be neglected in the expressions for the strain tensors, and material functions may be replaced by their linear approximations.

Substitution of Eq. (16) into Eqs. (20) and (40) implies that

$$\hat{F}(t,\tau) = \hat{G}(t,\tau) = \hat{I} + 2\hat{\epsilon}(t,\tau), \quad (78)$$

where

$$\hat{\epsilon}(t,\tau) = \frac{1}{2}\left[\bar{\nabla}(\tau)\bar{u}(t,\tau) + \left(\bar{\nabla}(\tau)\bar{u}(t,\tau)\right)^{\top}\right] \quad (79)$$

is the infinitesimal strain tensor for transition from the actual configuration at time τ to the actual configuration at time t.

Combining Eqs. (22) and (78) and bearing in mind the equality

$$\bar{l}\cdot\bar{l} = 1, \quad (80)$$

we obtain

$$\lambda(t,\tau,\bar{l}) = 1 + \bar{l}\cdot\hat{\epsilon}(t,\tau)\cdot\bar{l}. \quad (81)$$

The infinitesimal plastic strain is given by

$$\epsilon_p(t,\tau,\bar{l}) = \lambda_p(t,\tau,\bar{l}) - 1. \quad (82)$$

It follows from Eqs. (26), (81) and (82) that

$$\lambda_e(t,\tau,\bar{l}) = 1 + \bar{l}\cdot\hat{\epsilon}(t,\tau)\cdot\bar{l} - \epsilon_p(t,\tau,\bar{l}). \quad (83)$$

This equality together with Eq. (28) implies that with the required level of accuracy,

$$\frac{\mathrm{d}w_m^o}{\mathrm{d}\lambda}\left(\lambda_e(t,\tau,\bar{l})\right) = \frac{\mathrm{d}w_m^o}{\mathrm{d}\lambda}(1) + \frac{\mathrm{d}^2w_m^o}{\mathrm{d}\lambda^2}(1) \times\left[\bar{l}\cdot\hat{\epsilon}(t,\tau)\cdot\bar{l} - \epsilon_p(t,\tau,\bar{l})\right]$$

$$= \mu_m\left[\bar{l}\cdot\hat{\epsilon}(t,\tau)\cdot\bar{l} - \epsilon_p(t,\tau,\bar{l})\right], \quad (84)$$

where

$$\mu_m = \frac{\mathrm{d}^2w_m^o}{\mathrm{d}\lambda^2}(1). \quad (85)$$

Substitution of Eqs. (83) and (84) into Eq. (51) results in

$$\Sigma_m(t,\tau,\bar{l}) = \mu_m\left[\bar{l}\cdot\hat{\epsilon}(t,\tau)\cdot\bar{l} - \epsilon_p(t,\tau,\bar{l})\right]. \quad (86)$$

For isotropic materials, the rates of breakage and reformation, as well as the concentrations η_m of various kinds of links, are independent of $\bar{l}$:

$$\Gamma_{m0}(t,\bar{l}) = \Gamma_{m0}(t), \quad \Gamma_m(t,\tau,\bar{l}) = \Gamma_m(t,\tau).$$

Combining Eqs. (55) and (86), we find that

$$\Sigma(t,\tau,\bar{l}) = K(t,\tau)\left[\bar{l}\cdot\hat{\epsilon}(t,\tau)\cdot\bar{l} - \epsilon_p(t,\tau,\bar{l})\right], \quad (87)$$

where

$$K(t,\tau) = \sum_{m=1}^{M}\eta_m\mu_m\gamma_m(\tau)\exp\left[-\int_\tau^t\Gamma_m(s,\tau)\,\mathrm{d}s\right]. \quad (88)$$

At small strains, the Hencky plastic strain ε_p coincides with the infinitesimal plastic strain ϵ_p. Substituting Eq. (87) into the constitutive Eq. (71) and using the equality $\mathscr{H}(0) = 0$ that holds for any odd function, we obtain

$$\frac{\partial\epsilon_p}{\partial t}(t,\tau,\bar{l}) = H_0K(t,\tau)\left[\bar{l}\cdot\hat{\epsilon}(t,\tau)\cdot\bar{l} - \epsilon_p(t,\tau,\bar{l})\right], \quad (89)$$

where

$$H_0 = \frac{\mathrm{d}\mathscr{H}}{\mathrm{d}\Sigma}(0). \quad (90)$$

The initial condition for differential Eq. (89) reads

$$\epsilon_p(\tau,\tau,\bar{l}) = 0. \quad (91)$$

We seek a solution of Eqs. (89) and (91) in the form

$$\epsilon_p(t,\tau,\bar{l}) = \bar{l}\cdot\hat{\epsilon}_p(t,\tau)\cdot\bar{l}, \quad (92)$$

where $\hat{\epsilon}_p(t,\tau)$ is a tensor-valued function to be found. Substitution of Eq. (92) into Eqs. (89) and (91) results in

$$\frac{\partial\hat{\epsilon}_p}{\partial t}(t,\tau) = H_0K(t,\tau)[\hat{\epsilon}(t,\tau) - \hat{\epsilon}_p(t,\tau)], \quad \hat{\epsilon}_p(\tau,\tau) = 0. \quad (93)$$

For an incompressible medium, the first invariant of the infinitesimal strain tensor $\hat{\epsilon}$ vanishes,

$$I_1(\hat{\epsilon}(t,\tau)) = 0. \quad (94)$$

It follows from Eqs. (93) and (94) that

$$I_1\left(\hat{\epsilon}_p(t,\tau)\right) = 0, \quad (95)$$

which, together with Eq. (94), implies that

$$I_1(\hat{\varepsilon}(t,\tau)) = 0, \quad (96)$$

where

$$\hat{\varepsilon}(t,\tau) = \hat{\epsilon}(t,\tau) - \hat{\epsilon}_p(t,\tau). \quad (97)$$

Substitution of Eqs. (92) and (97) into Eq. (87) yields

$$\Sigma(t,\tau,\bar{l}) = K(t,\tau)\bar{l}\cdot\hat{\varepsilon}(t,\tau)\cdot\bar{l}. \quad (98)$$

It follows from Eqs. (16), (39), (78) and (98) that with the required level of accuracy,

$$\frac{\Sigma(t,\tau,\bar{l})}{\bar{l}\cdot\hat{G}(t,\tau)\cdot\bar{l}}\hat{\mathscr{F}}(t,\tau,\bar{l}) = K(t,\tau)\big[\bar{l}\cdot\hat{\varepsilon}(t,\tau)\cdot\bar{l}\big]\overline{ll}. \tag{99}$$

We introduce Cartesian coordinates $\{x_i\}$ with unit vectors $\bar{e}_i$ directed along the eigenvectors of the symmetrical tensor $\hat{\varepsilon}(t,\tau)$. The position of the unit vector $\bar{l}$ with respect to the Cartesian coordinate frame is determined by the spherical angles ϑ and φ:

$$\bar{l} = \cos\vartheta\bar{e}_1 + \sin\vartheta\big(\cos\varphi\bar{e}_2 + \sin\varphi\bar{e}_3\big). \tag{100}$$

The tensor $\overline{ll}$ is presented in the matrix form

$$\overline{ll} = \begin{bmatrix} \cos^2\vartheta & \sin\vartheta\cos\vartheta\cos\varphi & \sin\vartheta\cos\vartheta\sin\varphi \\ \sin\vartheta\cos\vartheta\cos\varphi & \sin^2\vartheta\cos^2\varphi & \sin^2\vartheta\sin\varphi\cos\varphi \\ \sin\vartheta\cos\vartheta\sin\varphi & \sin^2\vartheta\sin\varphi\cos\varphi & \sin^2\vartheta\sin^2\varphi \end{bmatrix}. \tag{101}$$

The tensor $\hat{\varepsilon}$ reads

$$\hat{\varepsilon} = \varepsilon_1\bar{e}_1\bar{e}_1 + \varepsilon_2\bar{e}_2\bar{e}_2 + \varepsilon_3\bar{e}_3\bar{e}_3, \tag{102}$$

where ε_n is the nth eigenvalue of $\hat{\varepsilon}$. It follows from Eqs. (100) and (102) that

$$\bar{l}\cdot\hat{\varepsilon}\cdot\bar{l} = \varepsilon_1\cos^2\vartheta + \Big(\varepsilon_2\cos^2\varphi + \varepsilon_3\sin^2\varphi\Big)\sin^2\vartheta. \tag{103}$$

Substituting Eqs. (101) and (103) into Eq. (99) and bearing in mind that

$$\mathrm{d}A(\bar{l}) = \sin\vartheta\,\mathrm{d}\vartheta\,\mathrm{d}\varphi, \tag{104}$$

we arrive at the formula

$$\int_{\mathscr{S}}\frac{\Sigma\hat{\mathscr{F}}}{\bar{l}\cdot\hat{G}\cdot\bar{l}}\,\mathrm{d}A = K\int_0^{\pi}\sin\vartheta\,\mathrm{d}\vartheta\int_0^{2\pi}\Big[\varepsilon_1\cos^2\vartheta + \Big(\varepsilon_2\cos^2\varphi + \varepsilon_3\sin^2\varphi\Big)\sin^2\vartheta\Big] \times\begin{bmatrix} \cos^2\vartheta & \sin\vartheta\cos\vartheta\cos\varphi & \sin\vartheta\cos\vartheta\sin\varphi \\ \sin\vartheta\cos\vartheta\cos\varphi & \sin^2\vartheta\cos^2\varphi & \sin^2\vartheta\sin\varphi\cos\varphi \\ \sin\vartheta\cos\vartheta\sin\varphi & \sin^2\vartheta\sin\varphi\cos\varphi & \sin^2\vartheta\sin^2\varphi \end{bmatrix}\mathrm{d}\varphi, \tag{105}$$

where arguments are omitted for simplicity. Calculating the integrals, we obtain

$$\int_{\mathscr{S}}\frac{\Sigma\hat{\mathscr{F}}}{\bar{l}\cdot\hat{G}\cdot\bar{l}}\,\mathrm{d}A = \frac{4\pi}{15}K \times\begin{bmatrix} 3\varepsilon_1+\varepsilon_2+\varepsilon_3 & 0 & 0 \\ 0 & \varepsilon_1+3\varepsilon_2+\varepsilon_3 & 0 \\ 0 & 0 & \varepsilon_1+\varepsilon_2+3\varepsilon_3 \end{bmatrix}.$$

This equality can be written as

$$\int_{\mathscr{S}}\frac{\Sigma(t,\tau,\bar{l})}{\bar{l}\cdot\hat{G}(t,\tau)\cdot\bar{l}}\hat{\mathscr{F}}(t,\tau,\bar{l})\,\mathrm{d}A(\bar{l}) = \frac{4\pi}{15}K(t,\tau)\big[I_1(\hat{\varepsilon}(t,\tau)) + 2\hat{\varepsilon}(t,\tau)\big]. \tag{106}$$

Eqs. (96), (97) and (106) imply that

$$\int_{\mathscr{S}}\frac{\Sigma(t,\tau,\bar{l})}{\bar{l}\cdot\hat{G}(t,\tau)\cdot\bar{l}}\hat{\mathscr{F}}(t,\tau,\bar{l})\,\mathrm{d}A(\bar{l}) = \frac{8\pi}{15}K(t,\tau)\hat{\varepsilon}(t,\tau) = \frac{8\pi}{15}K(t,\tau)[\hat{\boldsymbol{\epsilon}}(t,\tau) - \hat{\boldsymbol{\epsilon}}_p(t,\tau)]. \tag{107}$$

By analogy with Eq. (107), we can write

$$\int_{\mathscr{S}}\frac{\Sigma_0(t,\bar{l})}{\bar{l}\cdot\hat{G}_0(t)\cdot\bar{l}}\hat{\mathscr{F}}_0(t,\bar{l})\,\mathrm{d}A(\bar{l}) = \frac{8\pi}{15}K_0(t)[\hat{\boldsymbol{\epsilon}}_0(t) - \hat{\boldsymbol{\epsilon}}_{p0}(t)]. \tag{108}$$

Here

$$K_0(t) = \sum_{m=1}^{M}\eta_m\mu_m\exp\Big[-\int_0^t\Gamma_{m0}(s)\,\mathrm{d}s\Big], \tag{109}$$

$\hat{\boldsymbol{\epsilon}}_0(t)$ is the infinitesimal strain tensor for transition from the initial configuration to the actual configuration at time t, and the tensor $\hat{\boldsymbol{\epsilon}}_{p0}(t)$ obeys the ordinary differential equation [cf. Eq. (93)]

$$\frac{\mathrm{d}\hat{\boldsymbol{\epsilon}}_{p0}}{\mathrm{d}t}(t) = H_0K_0(t)[\hat{\boldsymbol{\epsilon}}_0(t) - \hat{\boldsymbol{\epsilon}}_{p0}(t)], \quad \hat{\boldsymbol{\epsilon}}_{p0}(0) = 0. \tag{110}$$

Substituting Eqs. (107) and (108) into the constitutive Eq. (77), we find that

$$\hat{\sigma}(t) = -p(t)\hat{I} + \frac{8\pi}{15}\rho\Xi\Big\{K_0(t)[\hat{\boldsymbol{\epsilon}}_0(t) - \hat{\boldsymbol{\epsilon}}_{p0}(t)] + \int_0^t K(t,\tau)[\hat{\boldsymbol{\epsilon}}(t,\tau) - \hat{\boldsymbol{\epsilon}}_p(t,\tau)]\,\mathrm{d}\tau\Big\}. \tag{111}$$

Without loss of generality, we can assume that the mechanical energies coincide for adaptive links of various kinds, which leads to the formula

$$\mu_1 = \ldots = \mu_M = \mu_0. \tag{112}$$

The infinitesimal strain tensor $\hat{\boldsymbol{\epsilon}}(t,\tau)$ for transition from

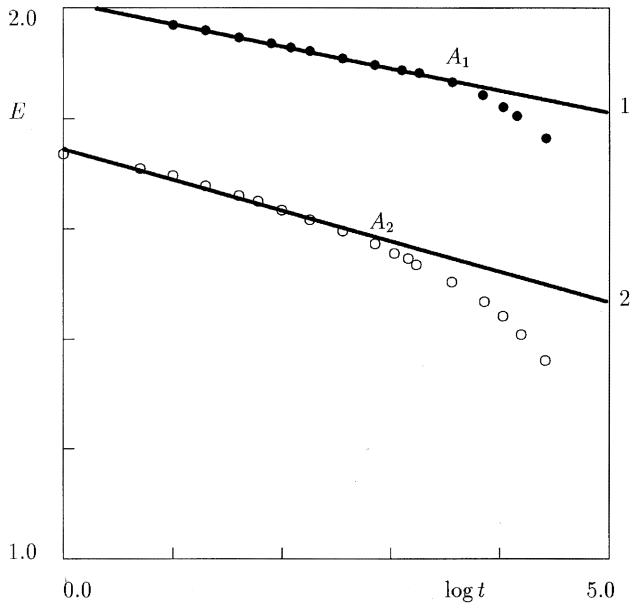

Fig. 1. The tensile relaxation modulus E (GPa) versus time t (s) for polycarbonate. Circles: experimental data obtained by Litt and Torp [45] in relaxation tests at 67°C. Filled circles: $\epsilon = 0.0193$; unfilled circles: $\epsilon = 0.0331$. Solid lines: their approximation by the linear function $E = c_1 + c_2 \log t$ with $c_1 = 2.0128$, $c_2 = -0.0404$ (curve 1) and $c_1 = 1.7447$, $c_2 = -0.0555$ (curve 2).

the actual configuration at time τ to the actual configuration at time t is calculated as

$$\hat{\epsilon}(t,\tau) = \hat{\epsilon}_0(t) - \hat{\epsilon}_0(\tau). \tag{113}$$

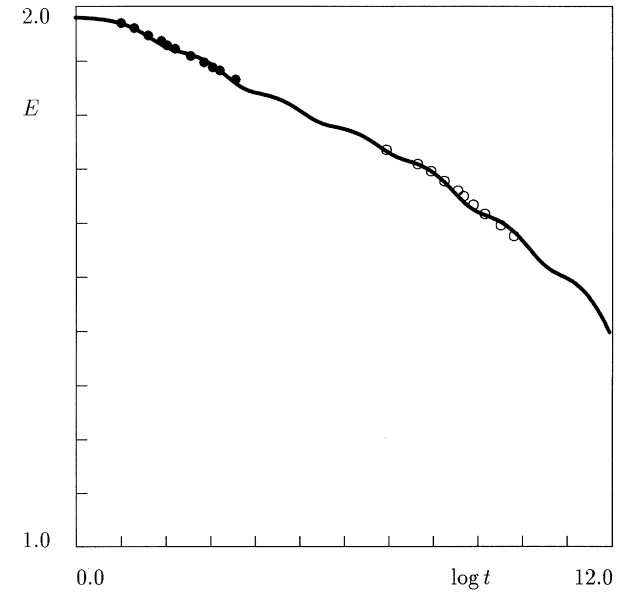

Fig. 2. The tensile relaxation modulus E (GPa) versus time t (s) for polycarbonate. Circles: treatment of experimental data obtained by Litt and Torp [45] in tensile relaxation test at 67°C. Filled circles: $\epsilon = 0.0193$; unfilled circles: $\epsilon = 0.0331$. Solid line: approximation of the relaxation master-curve (reduced to the reference strain $\epsilon_r = 0.0193$) with $M = 8$, $E_0 = 1.9815$ GPa, and the adjustable parameters Γ_{m^*} and η_m listed in Table 1.

Substitution of Eqs. (112) and (113) into Eq. (111) implies the linear constitutive equation in viscoelastoplasticity of polymers:

$$\hat{\sigma}(t) = -p(t)\hat{I} + 2\mu\Big\{K_0^*(t)[\hat{\epsilon}_0(t) - \hat{\epsilon}_{p0}(t)] + \int_0^t K^*(t,\tau)[\hat{\epsilon}_0(t) - \hat{\epsilon}_0(\tau) - \hat{\epsilon}_p(t,\tau)]\,d\tau\Big\}, \tag{114}$$

where

$$K_0^*(t) = \sum_{m=1}^{M} \eta_m \exp\Big[-\int_0^t \Gamma_{m0}(s)\,ds\Big],$$

$$K^*(t,\tau) = \sum_{m=1}^{M} \eta_m \gamma_m(\tau) \exp\Big[-\int_\tau^t \Gamma_m(s,\tau)\,ds\Big], \tag{115}$$

$$\mu = \frac{4\pi}{15}\rho\mu_0\Xi.$$

It follows from Eqs. (93), (110) and (113) that the infinitesimal plastic strain tensors $\hat{\epsilon}_{p0}(t)$ and $\hat{\epsilon}_p(t,\tau)$ satisfy the differential equations

$$\frac{d\hat{\epsilon}_{p0}}{dt}(t) = HK_0^*(t)[\epsilon_0(t) - \hat{\epsilon}_{p0}(t)],\ \hat{\epsilon}_{p0}(0) = 0,$$

$$\frac{\partial\hat{\epsilon}_p}{\partial t}(t,\tau) = HK^*(t,\tau)[\epsilon_0(t) - \hat{\epsilon}_0(\tau) - \hat{\epsilon}_p(t,\tau)],\ \hat{\epsilon}_p(\tau,\tau) = 0 \tag{116}$$

with

$$H = \mu_0 H_0. \tag{117}$$

7. Comparison with experimental data

Eqs. (114) and (116) determine the response of a linear, isotropic, incompressible, viscoelastoplastic medium under an arbitrary loading. For relaxation tests with

$$\hat{\epsilon}_0(t) = \begin{cases} 0, & t < 0, \\ \hat{\epsilon}_0, & t \geq 0, \end{cases} \tag{118}$$

these relationships can be simplified. Substitution of Eq. (118) into the second equality in Eq. (116) implies that for any $0 \leq \tau \leq t$,

$$\hat{\epsilon}_p(t,\tau) = 0. \tag{119}$$

The tensor function

$$\hat{\mathscr{E}}(t) = \hat{\epsilon}_0(t) - \hat{\epsilon}_{p0}(t) = \hat{\epsilon}_0 - \hat{\epsilon}_{p0}(t) \tag{120}$$

satisfies the differential equation

$$\frac{d\hat{\mathscr{E}}}{dt}(t) = -HK_0^*(t)\hat{\mathscr{E}}(t), \quad \hat{\mathscr{E}}(0) = \hat{\epsilon}_0. \tag{121}$$

Table 1
Adjustable parameters Γ_{m*} (s^{-1}) and η_m for polycarbonate at 67°C

Γ_{m*}	η_m
0.020 000 000 000 0000	0.0293
0.000 400 000 000 0000	0.0391
0.000 008 000 000 0000	0.0313
0.000 000 160 000 0000	0.0307
0.000 000 003 200 0000	0.0496
0.000 000 000 064 0000	0.0548
0.000 000 000 001 2800	0.0584
0.000 000 000 000 0256	0.7068

Resolving Eq. (121) with respect to $\hat{\mathscr{E}}(t)$, we find that

$$\hat{\mathscr{E}}(t) = \hat{\epsilon}_0 \exp\Big[-H\int_0^t K_0^*(\tau)\,d\tau\Big]. \quad (122)$$

Substitution of Eqs. (118), (120) and (122) into Eq. (114) implies that

$$\hat{\sigma}(t) = -p(t)\hat{I} + 2\mu\hat{\epsilon}_0 K_0^*(t)\exp\Big[-H\int_0^t K_0^*(\tau)\,d\tau\Big]. \quad (123)$$

For definiteness, we analyze uniaxial extension of a viscoelastoplastic bar. We introduce Cartesian coordinates $\{x_i\}$, where the axis x_1 coincides with the longitudinal axis of the specimen. According to the incompressibility condition, the strain tensor $\hat{\epsilon}_0$ is given by

$$\hat{\epsilon}_0 = \epsilon_0\bar{e}_1\bar{e}_1 - \frac{1}{2}\epsilon_0(\bar{e}_2\bar{e}_2 + \bar{e}_3\bar{e}_3), \quad (124)$$

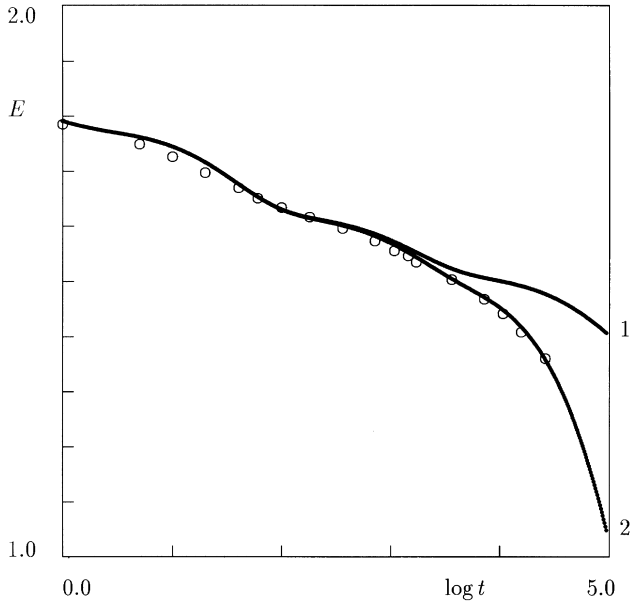

Fig. 4. The relaxation modulus E (GPa) versus time t (s) for polycarbonate. Circles: experimental data obtained by Litt and Torp [45] in tensile relaxation test with the strain $\epsilon_0 = 0.0331$ at 67°C. Solid lines: predictions of the model. Curve 1: viscoelastic material; curve 2: viscoelastoplastic material with $H(\epsilon_0) = 4.0 \times 10^{-6}\,s^{-1}$.

where ϵ_0 is the longitudinal strain, and $\bar{e}_i$ are unit vectors of the coordinate frame. Substitution of Eq. (124) into Eq. (123) implies that

$$\hat{\sigma}(t) = \sigma_1(t)\bar{e}_1\bar{e}_1 + \sigma_2(t)(\bar{e}_2\bar{e}_2 + \bar{e}_3\bar{e}_3), \quad (125)$$

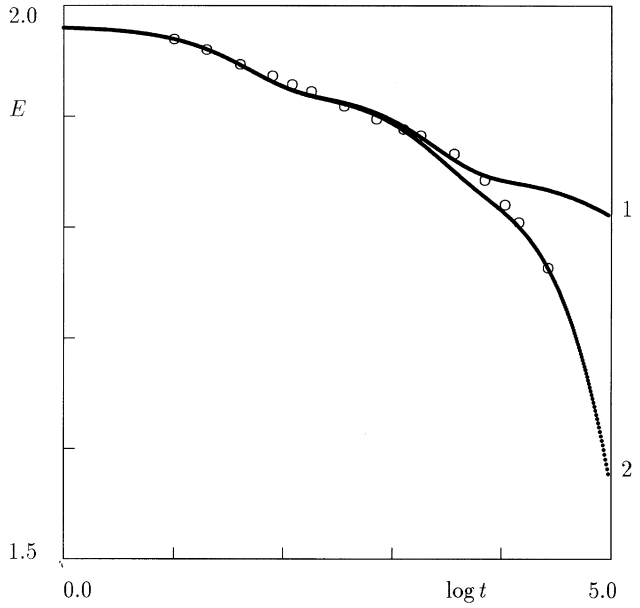

Fig. 3. The relaxation modulus E (GPa) versus time t (s) for polycarbonate. Circles: experimental data obtained by Litt and Torp [45] in tensile relaxation test with the strain $\epsilon_0 = 0.0193$ at 67°C. Solid lines: predictions of the model. Curve 1: viscoelastic material; curve 2: viscoelastoplastic material with $H(\epsilon_0) = 1.5 \times 10^{-6}\,s^{-1}$.

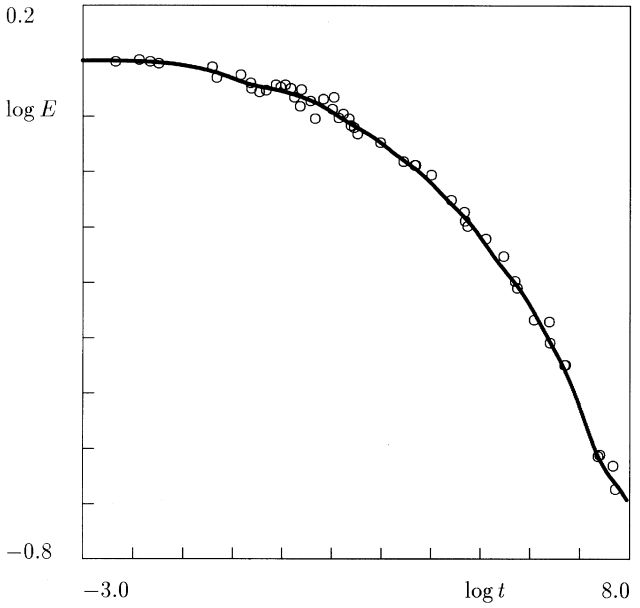

Fig. 5. The tensile relaxation modulus E (GPa) versus time t (s) for rubber-toughened poly(methyl methacrylate) at 70°C. Circles: treatment of experimental data obtained by Mariani et al. [49]. Solid line: approximation of the master-curve (reduced to $\epsilon_r = 0.001$) by Eq. (128) with $E_0 = 1.2624$ GPa, $M = 11$, and the adjustable parameters Γ_{m*} and η_m listed in Table 2.

Table 2
Adjustable parameters Γ_{m*} (s^{-1}) and η_m for rubber-toughened poly(methyl methacrylate) at 70°C

Γ_{m*}	η_m
10.000 000 000	0.0166
1.000 000 000	0.0763
0.100 000 000	0.0235
0.010 000 000	0.0968
0.001 000 000	0.0988
0.000 100 000	0.1078
0.000 010 000	0.1310
0.000 001 000	0.1074
0.000 000 100	0.1496
0.000 000 010	0.0243
0.000 000 001	0.1678

where

$$\sigma_1(t) = -p(t) + 2\mu\epsilon_0 K_0^*(t) \exp\left[-H\int_0^t K_0^*(\tau)\,d\tau\right],$$
$$\sigma_2(t) = -p(t) - \mu\epsilon_0 K_0^*(t) \exp\left[-H\int_0^t K_0^*(\tau)\,d\tau\right]. \quad (126)$$

Eq. (126) and the boundary condition on the lateral surface of the bar

$$\sigma_2(t) = 0$$

imply that the longitudinal stress is calculated as

$$\sigma_1(t) = E_0\epsilon_0 K_0^*(t) \exp\left[-H\int_0^t K_0^*(\tau)\,d\tau\right], \quad (127)$$

where

$$E_0 = 3\mu$$

is Young's modulus. For comparison, we provide the formula for the response of a linear viscoelastic medium (with $H = 0$)

$$\sigma_1(t) = E_0\epsilon_0 K_0^*(t). \quad (128)$$

It follows from Eqs. (127) and (128) that the material plasticity leads to an exponential decrease in the relaxation moduli; the rate of the decrease is determined by the rate of plastic flow H.

Eq. (127) predicts the longitudinal stress in a linear viscoelastoplastic material. However, it also remains valid for nonlinear viscoelastoplastic media at small strains, where the rates of breakage and reformation for adaptive links γ_m, Γ_{m0}, Γ_m, as well as the rate of plastic flow H, depend on strains.

Experimental data for glassy polymers obtained in standard relaxation tests at different strain levels (below the yield point, when the effect of plasticity can be neglected) show that relaxation curves plotted in double logarithmic coordinates can be superposed by shifts along the time-axis (the time–strain superposition principle). This phenomenon is conventionally explained by the presence of some internal (material) clock governing reformation of adaptive links. The time–strain superposition principle is equivalent to the assumption that the rates of breakage are functions of the strain tensor:

$$\Gamma_m^o|_{\epsilon=\epsilon_0} = \frac{\Gamma_{m*}^o}{a(\epsilon_0)}, \quad (129)$$

where Γ_{m*}^o is the rate of breakage for the mth kind of adaptive links at the reference strain ϵ_r and a is the relative shift factor.

Unlike nonlinear *viscoelastic* media, *viscoelastoplastic*

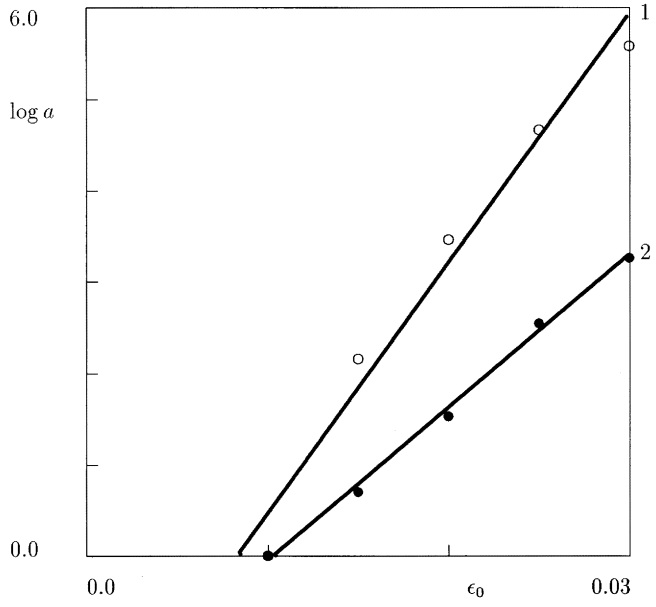

Fig. 6. The shift factor a versus the longitudinal strain ϵ_0 for rubber-toughened poly(methyl methacrylate). Circles: treatment of experimental data obtained by Mariani et al. [49]; Unfilled circles: $\Theta = 70$°C; filled circles: $\Theta = 90$°C. Solid lines: approximations of experimental data by Eq. (130) with $c = 273.56$ (curve 1) and $c = 167.02$ (curve 2).

Table 3
Adjustable parameters Γ_{m*} (s^{-1}) and η_m for rubber-toughened poly(methyl methacrylate) at 90°C

Γ_{m*}	η_m	
	Fig. 7	Fig. 8
10.000 000	0.1095	0.1077
1.000 000	0.0781	0.0869
0.100 000	0.1499	0.1112
0.010 000	0.0662	0.2055
0.001 000	0.2744	0.2304
0.000 100	0.1860	0.1436
0.000 010	0.0916	0.1148
0.000 001	0.0443	0.0000

materials do not permit relaxation master-curves to be constructed by shifts of short-term relaxation curves. As an example, we refer to experimental data for polycarbonate depicted in Fig. 1. For a detailed description of the experimental procedure, see Ref. [45].

Litt and Torp [45] have found that in tensile relaxation tests at various temperatures within the range from -63 to 26°C, the stress linearly decreases with the growth of the logarithm of time over five decades of time. This behavior is typical of polycarbonate, which is confirmed by independent data provided by other sources [46].

At elevated temperatures (e.g. 67°C), the decrease in the longitudinal stress is linear up to a certain point (points A_1 and A_2 in Fig. 1), and crucially accelerates after this point.

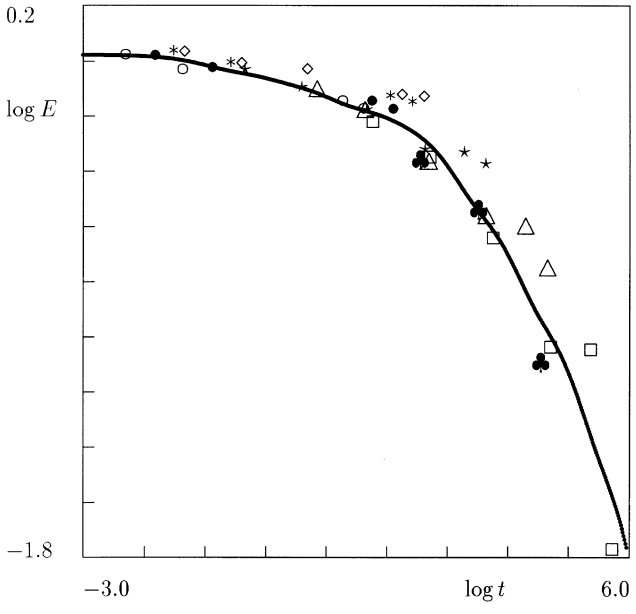

Fig. 7. The tensile relaxation modulus E (GPa) versus time t (s) for rubber-toughened poly(methyl methacrylate) at 90°C. Symbols: experimental data obtained by Mariani et al. [49]: ○ $\epsilon_0 = 0.001$; ● $\epsilon_0 = 0.003$; * $\epsilon_0 = 0.005$; ◇ $\epsilon_0 = 0.0075$; ★ $\epsilon_0 = 0.015$; △ $\epsilon_0 = 0.02$; □ $\epsilon_0 = 0.025$; ♣ $\epsilon_0 = 0.03$. Solid line: approximation of the master-curve (reduced to $\epsilon_r = 0.001$) by Eq. (128) with $E_0 = 1.0552$ GPa, $M = 8$, and the adjustable parameters Γ_{m*} and η_m listed in Table 3.

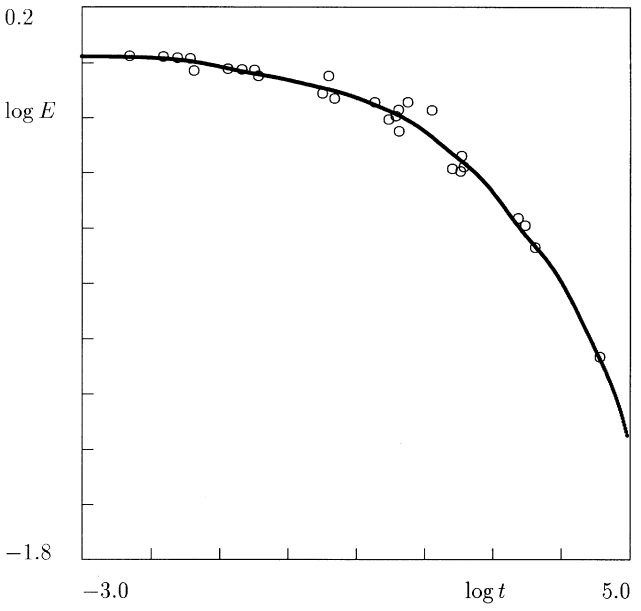

Fig. 8. The tensile relaxation modulus E (GPa) versus time t (s) for rubber-toughened poly(methyl methacrylate) at 90°C. Circles: treatment of experimental data obtained by Mariani et al. [49]. Solid line: approximation of the master-curve (reduced to $\epsilon_r = 0.001$) by Eq. (128) with $E_0 = 1.0550$ GPa, $M = 7$, and the adjustable parameters Γ_{m*} and η_m listed in Table 3.

The material softening exhibited in Fig. 1 is explained by the influence of material plasticity. This is in good agreement with observations carried out after static tests, which reveal considerable crazing of specimens [45].

Assuming that the effect of plasticity is insignificant at the initial intervals of measurements (that is H may be neglected before points A_i) and accepting the time–strain superposition principle Eq. (129), we find from Eq. (127) that the initial parts of the relaxation curves can be superposed by horizontal shifts. This hypothesis is confirmed fairly well by data plotted in Fig. 2, where experimental data obtained at $\epsilon_0 = 0.00331$ are shifted along the time-axis by 6.95 decades to construct a master-curve reduced to the reference strain $\epsilon_r = 0.00193$. The material parameters Γ_{m*} and η_m are collected in Table 1. The number M of relaxation times that approximate a continuous relaxation spectrum, as well as the relaxation rates Γ_{m*} reciprocal to the relaxation times are chosen to ensure an acceptable level of accuracy in fitting experimental data. Referring to Christensen [47], we choose M to coincide with the number of decades in a region on the time axis where experimental data are located. For a discussion of this issue, see also Ref. [48].

Given M, η_m, and Γ_{m*}, the values $H(\epsilon_0)$ are found to ensure the best fit of relaxation curves in the entire interval of measurements. Experimental data together with their approximations by the viscoelastic model (curves 1) and viscoelastoplastic model (curves 2) are plotted in Figs. 3 and 4. These figures show that the material plasticity significantly affects the relaxation curves, and its influence can be adequately predicted by quasi-linear constitutive Eqs. (114)

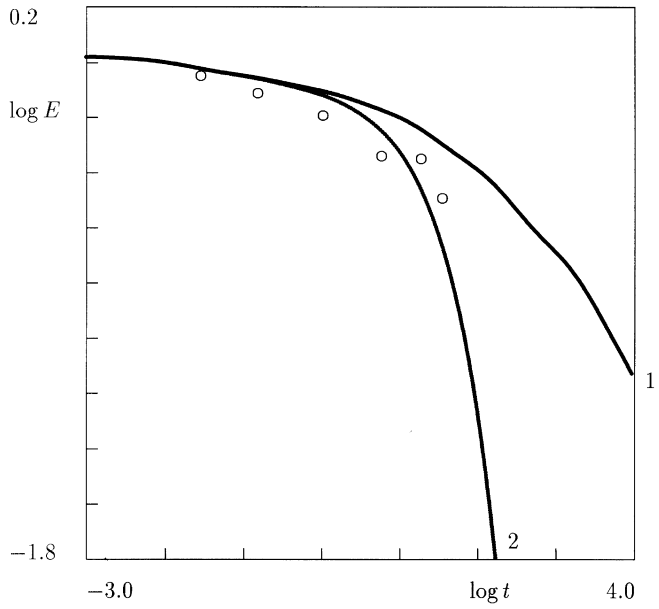

Fig. 9. The tensile relaxation modulus E (GPa) versus time t (s) for rubber-toughened poly(methyl methacrylate) at 90°C. Circles: experimental data obtained by Mariani et al. [49] at $\epsilon_0 = 0.015$. Solid lines: results of numerical simulation. Curve 1: the viscoelastic model; curve 2: the viscoelastoplastic model with $H = 0.04\ s^{-1}$.

and (116) with strain-dependent rates of breakage, reformation, and plastic flow.

To demonstrate that the constitutive equations can correctly describe experimental data for other polymers as well, we study relaxation curves for rubber-toughened poly(methyl methacrylate) measured at 70 and 90°C. For a detailed description of the experimental procedure, see Ref. [49].

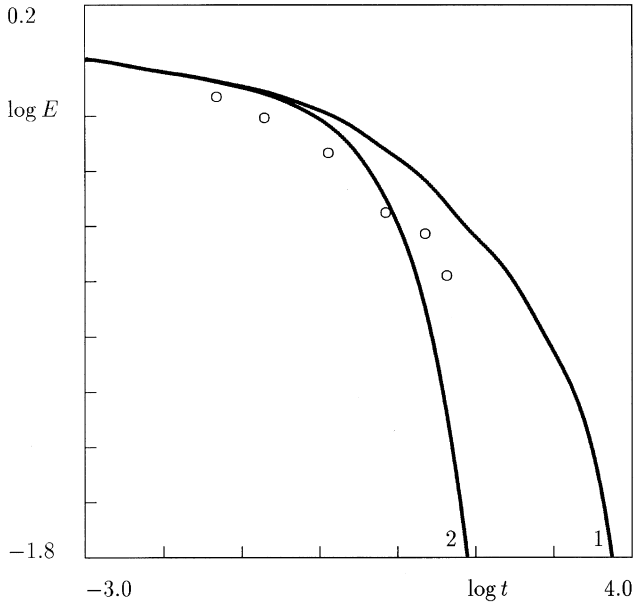

Fig. 10. The tensile relaxation modulus E (GPa) versus time t (s) for rubber-toughened poly(methyl methacrylate) at 90°C. Circles: experimental data obtained by Mariani et al. [49] at $\epsilon_0 = 0.02$. Solid lines: results of numerical simulation. Curve 1: the viscoelastic model; curve 2: the viscoelastoplastic model with $H = 0.10\ s^{-1}$.

The relaxation curves obtained at 70°C and plotted in double logarithmic coordinates can be superposed by horizontal shifts with a high level of accuracy. Fig. 5 presents experimental data shifted along the time axis and an approximation of the master-curve (reduced to the reference strain $\epsilon_r = 0.001$) by Eq. (128), where the function $K_0^*(t)$ is given by Eqs. (115) and (129) with the adjustable parameters Γ_{m*} and η_m collected in Table 2. The shift factor a is plotted versus the longitudinal strain ϵ_0 in Fig. 6, where experimental data are approximated by the dependence

$$\log a = c(\epsilon_0 - \epsilon_r), \quad \log = \log_{10}. \tag{130}$$

Results depicted in Figs. 5 and 6 imply that plastic effects may be neglected in specimens loaded at 70°C.

With an increase in temperature, the influence of material plasticity grows. This assertion is confirmed by experimental data obtained for poly(methyl methacrylate) at 90°C. An attempt to construct a master-curve by horizontal shifts of relaxation curves leads to significant deviations from the approximation of the tensile relaxation modulus E (adjustable parameters Γ_{m*} and η_m are collected in Table 3) (Fig. 7). Ascribing these discrepancies to the effect of plasticity, we find that only initial parts of the relaxation curves (which correspond to very small plastic strains) are superposable by horizontal shifts. A master-curve constructed by using 'truncated' relaxation curves is plotted in Fig. 8, which demonstrates excellent fit of experimental data.

The corresponding shift factor a is depicted in Fig. 6, which shows that Eq. (130) correctly predicts observations. This supports our model, since Eq. (130) is conventionally

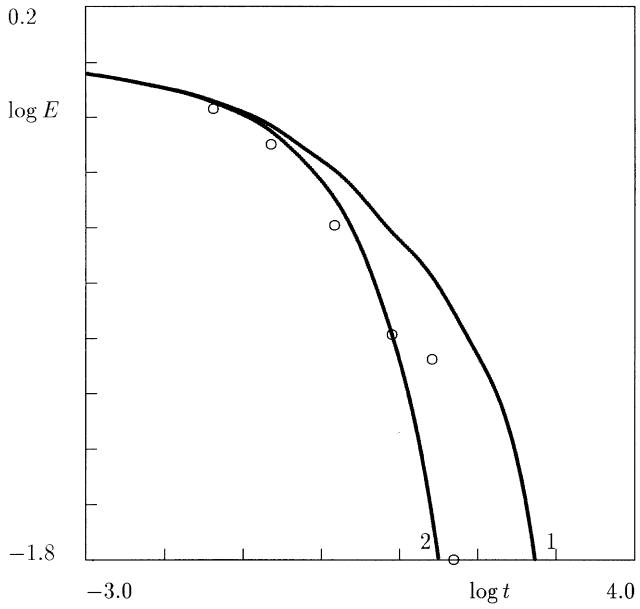

Fig. 11. The tensile relaxation modulus E (GPa) versus time t (s) for rubber-toughened poly(methyl methacrylate) at 90°C. Circles: experimental data obtained by Mariani et al. [49] at $\epsilon_0 = 0.025$. Solid lines: results of numerical simulation. Curve 1: the viscoelastic model; curve 2: the viscoelastoplastic model with $H = 0.31\ s^{-1}$.

employed to fit shift factors for nonlinear viscoelastic media.

To ensure an acceptable fit of the entire relaxation curves, we choose the rate of plastic strains H for any relaxation test with $\epsilon_0 > 0.01$. Results of numerical simulation are plotted together with experimental data in Figs. 9–12. These figures

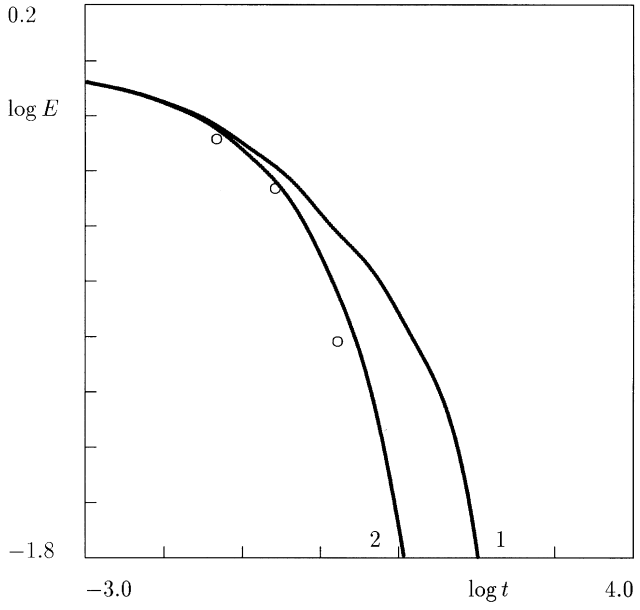

Fig. 12. The tensile relaxation modulus E (GPa) versus time t (s) for rubber-toughened poly(methyl methacrylate) at 90°C. Circles: experimental data obtained by Mariani et al. [49] at $\epsilon_0 = 0.03$. Solid lines: results of numerical simulation. Curve 1: the viscoelastic model; curve 2: the viscoelastoplastic model with $H = 0.90\ s^{-1}$.

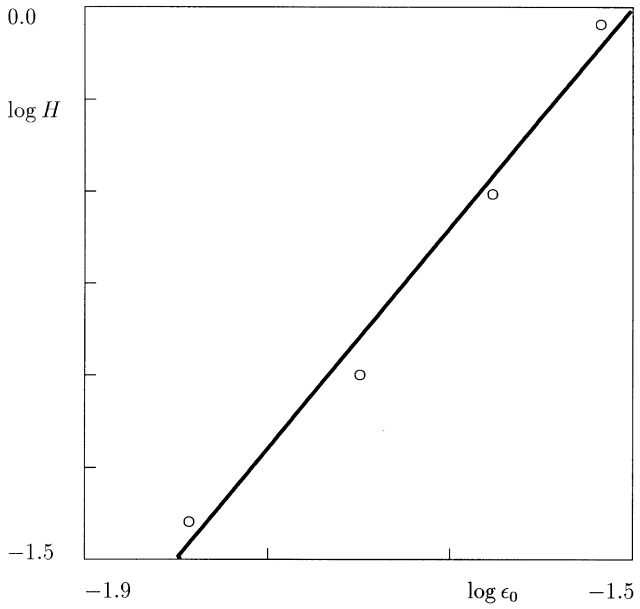

Fig. 13. The rate of plastic strains H versus the longitudinal strain ϵ_0 for rubber-toughened poly(methyl methacrylate). Circles: treatment of experimental data obtained by Mariani et al. [49]. Solid line: approximation of experimental data by Eq. (132) with $\log A = 6.7147$ and $\alpha = 4.4844$.

demonstrate fair agreement between observations and predictions of the model.

The dependence $H(\epsilon_0)$ is approximated by the power law

$$H = A\epsilon_0^{\alpha} \tag{131}$$

with two adjustable parameters A and α. It follows from Eq. (131) that the logarithm of the plastic rate of strain is a linear function of the logarithm of the longitudinal strain

$$\log H = \alpha \log \epsilon_0 + \log A. \tag{132}$$

Eq. (132) is fairly well confirmed by experimental data plotted in Fig. 13.

Figs. 5–13 show that the model may be applied not only to homogeneous materials, but also to polymeric composites. The conclusions drawn by fitting experimental data are in qualitative agreement with observations for other amorphous polymers, see for example, recent data for an epoxy resin in Ref. [50]. This may be explained as follows. Measurements by Mariani et al. [49] refer to a composite with relatively large rubber particles (the ratio of the average radius of a particle to the average radius of a cell is about 0.6), which means that the inhomogeneity in stress distribution across the cell (caused by the stress concentration at the interface) is rather weak and does not significantly affect relaxation times of the matrix. At small strains, when no detachment occurs at the interfaces, this allows the model to be employed in the study of particulate composites, where inclusions are treated as clusters of persistent links (analogous to chemical crosslinks in an amorphous polymer).

8. Concluding remarks

New constitutive equations have been derived for the viscoelastoplastic response of glassy polymers. The model is based on the concept of a temporary network, where adaptive links are treated as elastoplastic elements.

Explicit expressions are proposed for thermodynamic potentials of a transient network at finite strains. Constitutive equations are developed using the laws of thermodynamics. Nonlinear stress–strain relations with large deformations are simplified at small strains. Quasi-linear constitutive equations are derived for viscoelastoplastic polymers with strain-dependent rates of breakage, reformation, and plastic flow.

As examples, results of tensile relaxation tests are analyzed for polycarbonate at 67°C and rubber-toughened poly(methyl methacrylate) at 70 and 90°C. Adjustable parameters in the constitutive relations are found by fitting experimental data. It is demonstrated that the quasi-linear model correctly describes available experimental data and may be used to study stresses built up in polymeric articles.

Acknowledgements

Financial support by the Israeli Ministry of Science (grant 9641-1-96) is gratefully acknowledged.

References

[1] Ward IM. Mechanical properties of solid polymers. London: Wiley-Interscience, 1971.
[2] Fotheringham DG, Cherry BW. J Mater Sci 1978;13:951.
[3] Boyce MC, Parks DM, Argon AS. Mech Mater 1988;7:15.
[4] Eyring H. J Chem Phys 1936;4:283.
[5] Robertson RE. J Chem Phys 1966;44:3950.
[6] Haward RN, Thackray G. Proc R Soc Lond 1968;A302:453.
[7] Argon AS. Phil Mag 1973;A28:839.
[8] Argon AS, Bessonov MI. Phil Mag 1977;A35:917.
[9] Boyce MC, Parks DM, Argon AS. Int J Plasticity 1989;5:593.
[10] Boyce MC, Arruda EM. Polym Eng Sci 1990;30:1288.
[11] Wu PD, van der Giessen E. J Mech Phys Solids 1993;41:427.
[12] Hasan OA, Boyce MC. Polym Eng Sci 1995;35:331.
[13] Bauwens JC, Bauwens-Crowet C, Homes G. J Polym Sci A-2 1969;7:1745.
[14] Ree T, Eyring H. J Appl Phys 1955;26:793, 800.
[15] Bauwens-Crowet C, Bauwens JC, Homes G. J Polym Sci A-2 1969;7:735.
[16] Bauwens-Crowet C. J Mater Sci 1973;8:968.
[17] Povolo F, Schwartz G, Hermida EB. J Appl Polym Sci 1996;61:109.
[18] G'Sell C, Jonas JJ. J Mater Sci 1981;16:1956.
[19] Lefebvre JM, Escaig B. J Mater Sci 1985;20:438.
[20] Coulon G, Lefebvre JM, Escaig B. J Mater Sci 1986;21:2059.
[21] Caux X, Coulon G, Escaig B. Polymer 1988;29:808.
[22] Bordonaro CM, Krempl E. Polym Eng Sci 1992;32:1066.
[23] Kitagawa M, Zhou D, Qui J. Polym Eng Sci 1995;35:1725.
[24] Shay RM, Caruthers JM. J Rheol 1986;30:781.
[25] Wineman AS, Waldron WK. Polym Eng Sci 1993;33:1217.
[26] Wineman AS, Waldron WK. J Rheol 1995;39:401.
[27] Drozdov AD. J Rheol 1997;41:1223.
[28] Green MS, Tobolsky AV. J Chem Phys 1946;14:80.
[29] Yamamoto M. J Phys Soc Jpn 1956;11:413.
[30] Lodge AS. Rheol Acta 1968;7:379.
[31] Tanaka F, Edwards SF. Macromolecules 1992;25:1516.
[32] Drozdov AD. Eur J Mech A/Solids 1993;12:305.
[33] Drozdov AD. Rheol Acta 1995;34:562.
[34] Drozdov AD. Mech Res Commun 1997;24:161.
[35] Drozdov AD. Int J Solids Struct 1997;34:2685.
[36] Drozdov AD. Polym Eng Sci 1997;37:1983.
[37] Drozdov AD. Polymer 1998;39:1327.
[38] Tomita Y, Tanaka S. Int J Solids Struct 1995;32:3423.
[39] Treloar LRG. The physics of rubber elasticity. Oxford: Clarendon Press, 1975.
[40] Jones JL, Marques CM. J Phys France 1990;51:1113.
[41] Everaers R. J Phys II France 1995;5:1491.
[42] Drozdov AD. Finite elasticity and viscoelasticity. Singapore: World Scientific, 1996.
[43] Coleman BD, Gurtin ME. J Chem Phys 1967;47:597.
[44] Drozdov AD. Int J Solids Struct 1998;35:2315.
[45] Litt MH, Torp S. J Appl Phys 1973;44:4282.
[46] Ricco T, Smith TL. Polymer 1985;26:1979.
[47] Christensen RM. Theory of viscoelasticity. An introduction. New York: Academic Press, 1982.
[48] Soussou JE, Moavenzadeh F, Gradowszyk MH. Trans Soc Rheol 1970;14:573.
[49] Mariani P, Frassine R, Rink M, Pavan A. Polym Eng Sci 1996;36:2750.
[50] Cook WD, Mayr AE, Edward GH. Polymer 1998;39:3725.